

#### Contents lists available at ScienceDirect

## Petroleum Science





# Original Paper

Can clay-rich reservoirs in predominantly-freshwater lacustrine shale systems serve as primary exploration targets in low-medium maturity? A case study of the Triassic Yanchang Formation of the Ordos Basin



Enze Wang <sup>a,b,c</sup>, Maowen Li <sup>a,b,c,\*</sup>, Xiaoxiao Ma <sup>a,b,c</sup>, Menhui Qian <sup>a,b,c</sup>, Tingting Cao <sup>a,b,c</sup>, Zhiming Li <sup>a,b,c</sup>, Sen Li <sup>d</sup>, Zhijun Jin <sup>e</sup>

- <sup>a</sup> State Key Laboratory of Shale Oil and Gas Enrichment Mechanisms and Efficient Development, SINOPEC, Beijing, 102206, China
- b Key Laboratory of Shale Oil/Gas Exploration and Production Technology, SINOPEC, Beijing, 102206, China
- <sup>c</sup>Petroleum Exploration and Production Research Institute, SINOPEC, Beijing, 102206, China
- <sup>d</sup> China University of Geosciences (Wuhan), Wuhan, 430074, Hubei, China
- e Institute of Energy, Peking University, Beijing, 100871, China

#### ARTICLE INFO

#### Article history: Received 22 January 2025 Received in revised form 28 March 2025 Accepted 26 June 2025 Available online 7 July 2025

Edited by Xi Zhang and Jie Hao

Keywords: Lacustrine shale Lithofacies assemblages Clay-rich shale reservoirs Shale deposited in freshwater conditions Ordos Basin

#### ABSTRACT

Whether clay-rich shale reservoirs with low-medium maturity can serve as primary exploration targets remains a focal point of debate in the academic community. Clarifying the exploration potential of clayrich shale reservoirs is crucial for the future exploration and development of lacustrine shale. The Triassic Yanchang Formation in the Ordos Basin has been one of most productive lacustrine shale oil systems in China, with substantial oil production capacity already established. While the primary productive layers are currently fine-grained siltstone interbeds, however, it remains a highly debated issue whether the volumetrically more significant clay-rich reservoirs can become viable exploration targets in the near future. To address this issue, we examined the exploration potential of different lithofacies assemblages in Member 7 (Mbr 7) of the Triassic Yanchang Formation, using a borehole in the Tongchuan area of the southern Ordos Basin as an example. We identified favorable exploration targets and assessed whether clay-rich reservoirs formed predominantly-freshwater conditions can become viable exploration targets. The results indicate the presence of six lithofacies in clay-rich reservoirs of Mbr 7 of the Yanchang Formation, with two main lithofacies assemblages: laminated organic-rich shale and massive mudstone. From the perspective of sandstone distribution, the sandstone interlayers within laminated organic-rich shale are primarily formed by gravity (hyperpycnal) flows, while sandstones deposited in delta front environments are typically associated with massive mudstone. Laminated organic-rich shale deposition occurred in an anoxic, deep-water environment characterized by high primary productivity, whereas massive mudstone formed in environments with high sedimentation rates and substantial terrigenous debris influx. Currently, the exploration potential of sandstone interlayers exceeds that of clay-rich reservoirs, with the greatest potential observed in the sandstone interlayers associated with laminated organic-rich shale formed by gravity (hyperpycnal) flows. Comparative analysis reveals that clay-rich reservoirs with low to medium maturity present great challenges for exploitation, making interlayer-type reservoirs the main focus of exploration at this stage. Nevertheless, clay-rich reservoirs in closed systems with high thermal maturity and organic matter content also hold considerable potential.

© 2025 The Authors. Publishing services by Elsevier B.V. on behalf of KeAi Communications Co. Ltd. This is an open access article under the CC BY license (http://creativecommons.org/licenses/by/4.0/).

## \* Corresponding author.

E-mail address: limw.syky@sinopec.com (M. Li).

Peer review under the responsibility of China University of Petroleum (Beijing).

#### 1. Introduction

Shale oil, a type of unconventional oil and gas, holds immense resource potential (Jarvie, 2012; Katz and Lin, 2014; Li et al., 2021;

Wang et al., 2022; Hu et al., 2022). For instance, in the United States, shale oil (tight oil) accounted for 64% of oil and gas production in 2023, approximately 3.04 billion barrels (EIA, 2024). Previous research has estimated the global low-medium maturity shale oil resources at approximately 4823 billion barrels (Kang et al., 2020), with the resource amount of lacustrine shale reservoirs with low-medium maturity in the China is about 333 billion barrels. Although low-medium maturity lacustrine shale reservoirs exhibit enormous resource potential, current developments have predominantly targeted medium-high maturity (Zhao et al., 2024). The exploration viability and economic potential of lacustrine shale reservoirs with low-medium maturity remain contentious topics within the academic community.

Based on the lithological types and combinations, lacustrine shale plays can be categorized into three types: interlayer-type, clay-rich type, and mixed-type reservoirs (Katz and Lin, 2014; Guo et al., 2023; Jin et al., 2023; Sun et al., 2023; Cao et al., 2024). Although there remains no universally accepted definition for clay-rich shale reservoirs, shale systems deposited in freshwater environments typically exhibit elevated clay mineral content. For instance, the Jurassic Ziliujing Formation in the Sichuan Basin demonstrates an average clay mineral content of 48.7% (Wang et al., 2023a). Additionally, the Cretaceous Qingshankou Formation black shale in the Gulong Sag of Songliao Basin contains clay mineral contents ranging from 35% to 45% (Guo et al., 2023). Therefore, herein, we define the shale reservoirs with mean clay mineral content exceeding 40% as clay-rich type reservoirs. Compared to interlayer-type and mixed-type reservoirs, clay-rich reservoirs face skepticism in the industrial community regarding their potential for commercial development due to their relatively low matrix permeability and fracability. However, recent exploration efforts in clay-rich shale reservoirs have achieved industrial oil and gas flows in the Cretaceous Qingshankou Formation of the Songliao Basin (Sun et al., 2021). Yet, do these exploration successes suggest that clay-rich reservoirs in other lacustrine shale systems also hold the potential for breakthroughs? This remains uncertain.

Lithofacies are formed in specific sedimentary environments and exhibit variations owing different sedimentary settings, hydrocarbon generation processes, and diagenetic conditions (Loucks and Ruppel, 2007; Gamero-Diaz et al., 2013; Han et al., 2016; Iqbal et al., 2021; Ma et al., 2022; Feng et al., 2023a, 2023b). Numerous classification schemes and lithofacies division approaches have been proposed for shales from various perspectives by different scholars (Potter et al., 1980; O'Brien and Slatt, 1990; Loucks and Ruppel, 2007; Nichols, 2013; Abouelresh and Slatt, 2012; Lazar et al., 2015). However, prior studies on shale lithofacies classification have predominantly focused on shales formed in marine environments (Potter et al., 1980; Loucks and Ruppel, 2007; Abouelresh and Slatt, 2012; Lazar et al., 2015), with relatively limited attention given to lacustrine shales. Owing depositional environment differences, there are distinct geological characteristics existing between lacustrine and marine shales (Bohacs et al., 2000; Katz and Lin, 2014). Thus, whether existing shale lithofacies classification schemes are suitable for lacustrine shale plays remains a matter of debate. Currently, a unified lithofacies classification scheme for lacustrine shale plays remains to be established (Jin et al., 2023). With ongoing research, a relatively convergent classification approach is emerging within the academic community for lacustrine shales, highlighting the classification of lithofacies from the perspectives of mineral composition, sedimentary structures, and organic matter content (Li et al., 2022a; Ma et al., 2022; Wang et al., 2023c; Fan et al., 2024; He et al., 2024). However, studies that rigorously examine lithofacies with these essential geological parameters is scarce,

thereby hindering a comprehensive understanding of lithofacies characteristics across different lacustrine shale systems.

The Triassic Yanchang Formation of the Ordos Basin develops a set of organic-rich shales in oil window, and due to favorable geological conditions, it is one of the primary targets for lacustrine shale oil exploration and development in China (Zhang et al., 2017, 2023; Xu et al., 2019; Zhao et al., 2020a; Wang et al., 2024b). Meanwhile, it represents a typical lacustrine shale system deposited under freshwater conditions, where clay-rich and interlayertype shale reservoirs are widely developed. Nevertheless, the main productive layers of the Yanchang Formation are sandstone reservoirs (interlayer-type reservoirs, Jin et al., 2022; Wang et al., 2024b), leading some scholars to classify the Yanchang Formation as tight oil reservoirs rather than lacustrine shale plays. Due to the rapid decline in production rates characteristic of shale oil and gas plays (Hughes, 2013), petroleum explorers have shifted their focus to the clay-rich reservoirs that are widely developed in the Yanchang Formation to meet production continuity needs. This raises an important scientific question: can these clay-rich reservoirs with low to medium maturity serve as favorable exploration targets? Furthermore, due to the strong heterogeneity of lacustrine shale systems, the exploration potential differences between various lithofacies assemblages within clay-rich reservoirs remain

To address these questions, we examined Mbr 7 of the Yanchang Formation in the Ordos Basin. Here, we select a borehole in the southern Ordos Basin as an example, to classify systematically the lithofacies (lithofacies assemblages) of Mbr 7 of the Yanchang Formation, and explore the sedimentary environmental differences between various clay-rich reservoirs. In addition, we aim to clarify the exploration potential of various lithofacies assemblages in Mbr 7 of the Yanchang Formation, identify favorable exploration targets, and reveal whether clay-rich reservoirs formed predominantly-freshwater conditions can become viable exploration targets. The findings from this study provide a foundation for the exploration and development of shale plays within the Triassic Yanchang Formation of the Ordos Basin and contribute to a deeper understanding of the exploration potential of clay-rich reservoirs in other petroliferous basins.

### 2. Geological setting

The Ordos Basin, a significant petroliferous basin in China, spans an area of 320,000 km² (Fig. 1(a), Yang and Loon, 2022). It has a 4–5 km thick sedimentary succession from the Meso-Neoproterozoic to the Neogene on a stable Archean crystalline basement. While faults and folds are prevalent along the margins of the basin, the central part of the basin remains tectonically stable. The Mesoproterozoic to Early Paleozoic mainly features marine carbonate platform facies, transitioning to a marine–continental environment during the Late Paleozoic. The Mesozoic predominantly comprises lacustrine deposits, shifting to fluvial deposits in the Cenozoic.

The Yanchang Formation includes parts of the Middle Triassic and complete Upper Triassic, and the depositional facies of the Triassic Yanchang Formation in the Ordos Basin include deep and shallow lakes; braided, anastomosing, and meandering rivers; as well as delta plains and fronts (Fig. 1(b)–Qiao et al., 2021). These diverse depositional settings result in considerable lithological variations within the Triassic Yanchang Formation. Based on lithology, the Triassic Yanchang Formation is classified into 10 members (Deng et al., 2018). Paleontological analysis revealed that during the deposition of the Yanchang Formation, the basin was in a warm and humid low-latitude environment (Ji et al., 2010), with water salinity experiencing slight fluctuations but generally

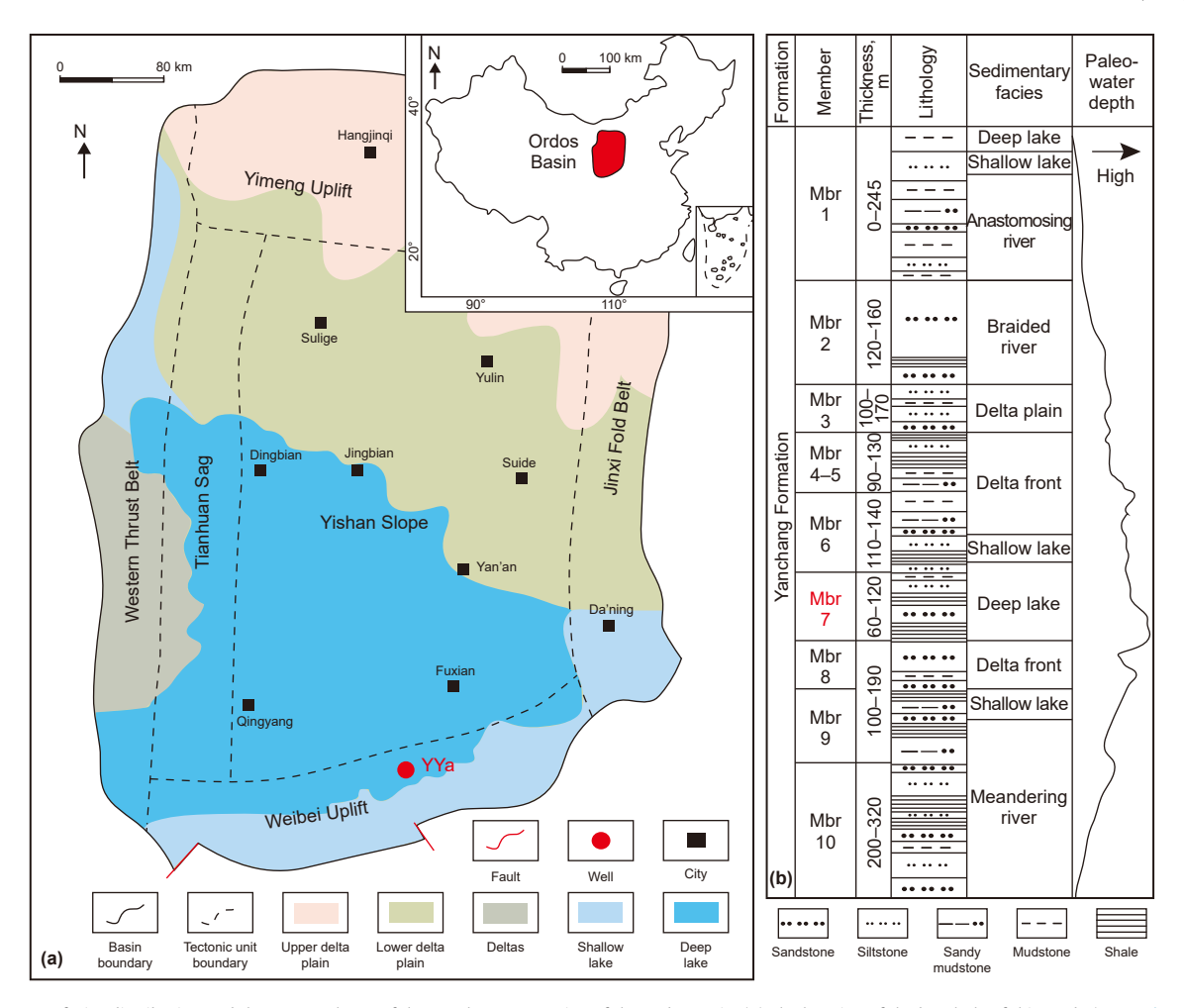


**Fig. 1.** Sedimentary facies distribution and the strata column of the Yanchang Formation of the Ordos Basin. (a) The location of the borehole of this study (From Chen et al., 2017). (b) Strata column of the Yanchang Formation in the Ordos Basin (Modified by Qiao et al., 2021).

remaining low. The deposition of Mbr 7 of the Yanchang Formation exhibited the highest paleodepth, resulting in the formation of organic-rich mudstones and shales (Zhao et al., 2020a). This study focused on the Tongchuan area in the southern Ordos Basin (Fig. 1 (a)), where the lithology of Mbr 7 of the Yanchang Formation is mainly dark-gray mudstone and black shale.

#### 3. Data and methods

## 3.1. Samples and experiments

Our study involved boreholes from several study areas in the Ordos Basin; in this study, we report only the data from the YYa borehole, which has the most comprehensive information. The samples were collected from the YYa borehole in the Ordos Basin, and their lithology includes sandstone, black shale, and mudstone, as shown in Fig. 2. All samples originated from Mbr 7 of the Yanchang Formation. The samples underwent X-ray diffraction (XRD), total organic carbon (TOC) analysis, organic petrological observation, vitrinite reflectance ( $R_0$ ) measurements, pyrolysis, and laser scanning confocal microscopy (LSC). All experiments were conducted at the SINOPEC Wuxi Institute of Petroleum Geology.

To conduct XRD testing, an Ultima IV diffractometer was used, operating at 40 kV and 40 mA. The samples were prepared by crushing and grinding the rock chips to a fine powder, passing

them through a 200-mesh sieve, and then mounting them on glass slides for analysis. The XRD patterns were collected over a  $2\theta$  range of  $5^{\circ}$ – $45^{\circ}$ . Notably, the traditional peak intensity comparison method was employed, not the Rietveld refinement method.

Before TOC analysis, the samples were crushed to 200 mesh and treated with hydrochloric acid, followed by washing with distilled water and drying at 80  $^{\circ}$ C for 4 h in a thermostatic oven. The TOC content was measured using a Leco CS230 carbon/sulfur analyzer.

Rock-Eval pyrolysis was performed on core samples ground to a grain size of less than 0.2 mm, using the Rock-Eval 6 standard model. The initial pyrolysis temperature was set to 300 °C and maintained for 3 min to generate the  $S_1$  peak. Then, the temperature was programmed to increase at a rate of 25 °C/min to a maximum of 650 °C, capturing the  $S_2$  peak.

Organic petrological observation was performed using a Leica DM4500P polarizing microscope equipped with a 50  $\times$  oil immersion objective to identify maceral compositions. The samples were impregnated with epoxy resin and, after curing, subjected to coarse and fine grinding to achieve a flat, smooth surface. Final polishing was performed using a 0.05- $\mu m$  alumina polishing agent. During observation, the macerals in the samples were examined under both white light and fluorescence modes. For the  $R_{\rm O}$  measurements, a minimum of 50 measurements were taken on vitrinite particles for every sample, and the mean reflectance value was calculated.

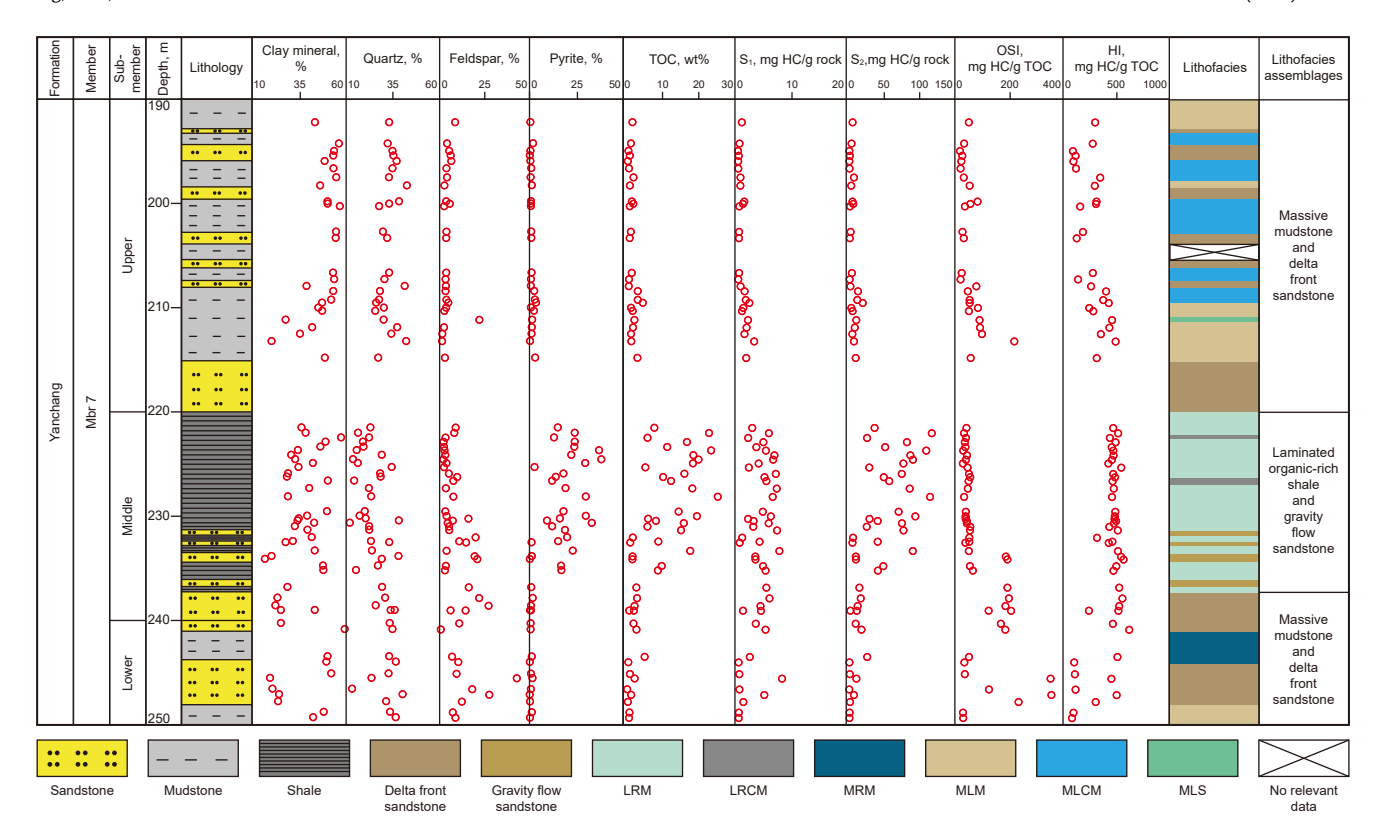


Fig. 2. Column showing the variations of lithology, mineral composition, TOC content, bulk geochemical and lithofacies development features of the Mbr 7 of the Yanchang Fm sedimentary rocks in the YYa borehole.

In this study, LSC was employed to observe the oil occurrence state. Before the experiment, the samples were polished to a mirrorlike finish to ensure optimal imaging conditions. The experimental equipment used was a Leica TCS SP5 system, equipped with a  $20\times$  objective lens, providing a spatial resolution of approximately 0.5  $\mu m$ . A laser wavelength of 488 nm was applied as the excitation source; fluorescence signals in the wavelength range of 500–590 nm represented light components of crude oil ( $C_{18}^-$ ), whereas signals from 590 to 800 nm represented heavy components ( $C_{18}^+$ ). The temperature was maintained at 22  $\pm$  1 °C throughout the experiment.

#### 3.2. Lithofacies classification standard

At present, there is no standardized system for classifying lacustrine shale lithofacies, but the academic community is converging on commonly accepted methods. The widely accepted classification typically considers three aspects: mineral composition, TOC content, and sedimentary textures (Loucks and Ruppel, 2007; Gamero-Diaz et al., 2013; Liang et al., 2017; Liu et al., 2019; Iqbal et al., 2021; Li et al., 2022a; Jin et al., 2023). As regards mineral composition, if siliceous, clay, or carbonate minerals exceed 50% of the shale, it is categorized as siliceous, argillaceous, or calcareous, respectively. If the content of these three minerals is <50%, the mineral composition is considered to be mixed shale. As regards the TOC content, as Mbr 7 of the Yanchang Formation sedimentary rocks generally exhibit high TOC content, this study used a TOC value of 5% to distinguish between organicrich and organic-lean sedimentary rocks. Lastly, regarding sedimentary texture, according to Li et al. (2022a), the textures were classified into laminated, banded, and massive types, reflecting the different hydrodynamic conditions during deposition.

#### 3.3. Kerogen type index

To quantify the kerogen type in lacustrine shale, this study references the type index (TI) obtained from organic petrographical analysis (Wang et al., 2023a). The calculation method is shown in Eq. (1). In general, TI values of less than 0, 0–40, 40–80, and more than 80 represent type I, II<sub>1</sub>, II<sub>2</sub>, and III kerogens, respectively.

$$TI = \frac{A \times 100 + L \times 50 + V \times (-75) + I \times (-100)}{100}$$
 (1)

where *A*, *L*, *V*, and *I* denote the proportions of alginite, liptinite vitrinite, and inertinite in the kerogen, respectively.

#### 4. Results

# 4.1. Lithology, mineral composition, sedimentary texture, and lithofacies assemblage identification

Based on the lithological difference in Mbr 7 of the Yanchang Formation sedimentary rocks in the YYa borehole (Fig. 2), Mbr 7 can be divided into three submembers. The upper and lower submembers share similar lithologies, characterized by dark-gray mudstone interbedded with fine sandstone. Contrarily, the middle submember predominantly comprises black shale interbedded with fine sandstone. While sandstone interlayers are present across all submembers, their formation processes differ. Fu et al. (2021) identified two main types of sandstone interlayers in Mbr 7 of the Yanchang Formation: gravity flow and delta front interlayers. In addition, Jin et al. (2022) observed that hyperpycnal flow-induced sandstone interlayers are present in the deep-water settings of the Yanchang Formation. Overall, the interlayers formed by gravity (hyperpycnal) flow are typically associated with

deep-water environments and commonly coexist with black shale. As regards the thickness of these interlayers, delta front interlayers generally exhibit greater thickness than those formed by gravity (hyperpycnal) flow. In addition, sedimentary structures can serve as indicators of sandstone provenance, with sandstones deposited by gravity flow typically exhibiting normal grading characteristics.

The mineral composition of Mbr 7 of the Yanchang Formation sedimentary rocks in the YYa borehole is presented in Fig. 2. Considering that the aforementioned lithofacies classification approach is specifically tailored for shale and mudstone, the mineralogical characteristics reported herein solely pertain to the black shale and dark-gray mudstone of Mbr 7 of Yanchang Formation. In general, the sedimentary rock predominantly comprises clay minerals, with a range of 20.1%–57.3% (average of 43.5%). Quartz is the second most abundant mineral, ranging from 12.0% to 45.8%, (average of 27.6%), followed by a relatively minor content of feldspar, ranging from 1.5% to 21.3% (average of 5.3%). Notably, there is considerable variation in pyrite content among the samples, ranging from trace amounts (less than 1%) to 38.3% (average of 10.5%). Pyrite is generally enriched within the black shale of the middle submember of Mbr 7 of the Yanchang Formation.

There are discernible disparities in the mineral composition between black shale and dark-gray mudstone. Dark-gray mudstone typically exhibits greater quantities of clay minerals and quartz compared with black shale, whereas black shale contains notably higher amounts of pyrite than dark-gray mudstone. The TOC content in Mbr 7 of the Yanchang Formation shale and mudstone ranges from 0.73 to 25.25 wt% (with an average of 7.65 wt%). From a lithological standpoint, the TOC content in black shale (averaging 13.93 wt%) is considerably higher than that in dark-gray mudstone (averaging 1.81 wt%).

As regards the sedimentary texture, Mbr 7 of the Yanchang Formation sedimentary rocks within the YYa borehole mainly displays two distinct types: laminated and massive textures. The distribution of these textures varies depending on the lithology. Specifically, dark-gray mudstone frequently exhibits a massive

texture (Fig. 3(a) and (b)), characterized by the absence of any discernible directional mineral alignment. Contrarily, black shale commonly exhibits a laminated texture (Fig. 3(c), (d), (e), and (f)).

Based on the mineral composition, TOC content, and sedimentary texture, six distinct lithofacies can be identified in Mbr 7 of the Yanchang Formation shale and mudstone. These lithofacies include laminated organic-rich mixed shale (LRM), massive organic-rich mixed mudstone (MRM), laminated organic-rich argillaceous shale (LRCM), massive organic-lean mixed mudstone (MLM), massive organic-lean argillaceous mudstone (MLCM), and massive organic-lean siliceous mudstone (MLS). According to the lithofacies characteristics, these can be further grouped into two lithofacies assemblages: laminated organic-rich shale and massive mudstone. LRM and LRCM mainly develop in laminated organicrich shale, whereas MRM, MLM, MLCM, and MLS belong to massive mudstone. In terms of vertical distribution, LRM is the dominant lithofacies within laminated organic-rich shale, whereas massive mudstone is mainly represented by MLM and MLCM. Previous studies have generally divided Mbr 7 of the Yanchang Formation into two lithofacies: black shale and dark-gray mudstone (e.g., Zhao et al., 2020b). In this study, black shale and dark-gray mudstone corresponded more closely to lithofacies assemblages, with laminated organic-rich shale comparable to black shale and massive mudstone analogous to previous descriptions of dark-gray mudstone. It is essential to emphasize that different lithofacies assemblages are associated with sandstones formed through distinct depositional mechanisms. Typically, interlayers formed by gravity (hyperpycnal) flow are associated with laminated organic-rich shale, whereas sandstones deposited in delta front environments are adjacent to massive mudstone. These varying formation mechanisms of sandstones also result in variations in sandstone-strata thickness ratios across lithofacies assemblages. Within the layers dominated by laminated organic-rich shale, the sandstone-strata thickness ratio is 14.4%, whereas in the two layers dominated by massive mudstone, the sandstone-strata thickness ratios are 35.1% and 63.0%, respectively.

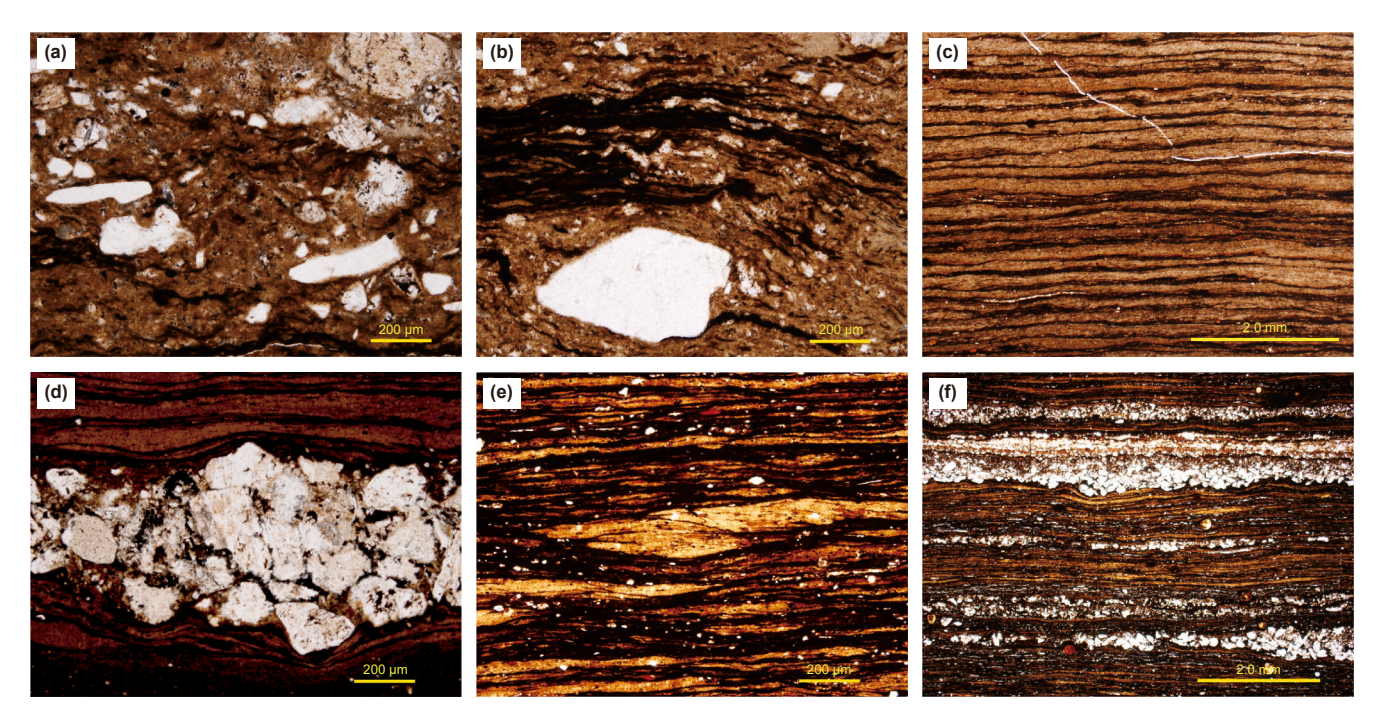


Fig. 3. Sedimentary textures of the Mbr 7 of the Yanchang Fm in YYa borehole. (a) 211.80 m, dark-gray, massive texture; (b) 211.06 m, dark-gray mudstone, massive texture; (c) 229.60 m, black shale, laminated texture; (d) 228.44 m, black shale, lenticular quartz; (e) 229.50 m, black shale, laminated texture; (f) 229.60 m, black shale, laminated texture.

#### 4.2. Bulk geochemical features

The  $S_1$  values of Mbr 7 of the Yanchang Formation shale and mudstone range from 0.09 to 7.68 mg HC/g rock (average 2.80 mg HC/g rock). The  $S_2$  values range from 0.50 to 117.22 mg HC/g rock (average 34.78 mg HC/g rock). The hydrogen index (HI) ranges from 64.94 to 543.45 mg HC/g TOC (average 366.64 mg HC/g TOC), and the oil saturation index (OSI) ranges from 12.00 to 215.71 mg HC/g TOC (average 41.80 mg HC/g TOC). Conversely, the TI values range from -53.9 to 62.5. According to the TOC content and pyrolysis parameters (Fig. 4), Mbr 7 of the Yanchang Formation shale and mudstone in the YYa borehole were mainly classified as fair to good source rocks. Notably, all samples of laminated organic-rich shale and most samples of massive mudstone were categorized as good source rocks, whereas only a few samples of massive mudstone were classified as fair source rocks.

Based on pyrolysis data, the kerogen types in Mbr 7 of the Yanchang Formation shale and mudstone are predominantly types II<sub>1</sub> and II<sub>2</sub>, with a minor presence of type III. The kerogen in laminated organic-rich shale is mainly type II<sub>1</sub>, whereas in massive mudstone, it is mainly type II<sub>2</sub> (Fig. 5).

The geochemical characteristics of the shale and mudstone across different lithofacies are summarized in Table 1. Organic-rich lithofacies exhibit elevated  $S_1$ ,  $S_2$ , and HI values than organic-lean lithofacies. However, organic-lean lithofacies exhibit higher OSI values relative to their organic-rich counterparts. Sandstone interlayers associated with different lithofacies assemblages are characterized by elevated  $S_1$  and OSI values but show lower  $S_2$  and HI values. In addition, in terms of kerogen type, the TI index is notably higher in laminated organic-rich shale than in massive mudstone.

### 4.3. Organic petrographic and oil occurrence features

The organic petrographic observations of Mbr 7 of the Yanchang Formation shale and mudstone within the YYa borehole, as shown in Fig. 6, indicate significant variations in kerogen types between the two lithofacies assemblages. In the laminated organic-rich shale samples, the kerogen contains abundant alginite, demonstrating bright yellow fluorescence (Fig. 6(a) and (b)). Conversely, the massive mudstone samples mainly comprise vitrinite and inertinite, with minimal alginite and liptinite contents (Fig. 6(c) and (d)), consistent with the trends observed in the pyrolysis parameters. The Ro values in the YYa borehole range from 0.68 to 0.74% (average 0.71%), suggesting that Mbr 7 of the Yanchang Formation in the YYa well is in the mature stage.

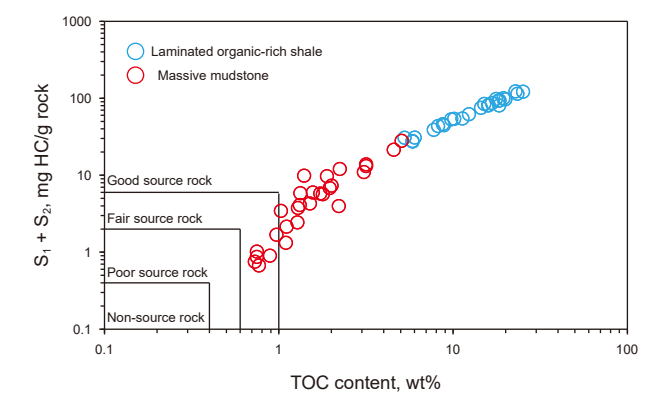


**Fig. 4.** TOC content and pyrolysis data of the Mbr 7 of the Yanchang Formation in YYa borehole, demonstrating that the laminated organic-rich shale samples exhibit better source rock quality compared to the massive mudstone samples.

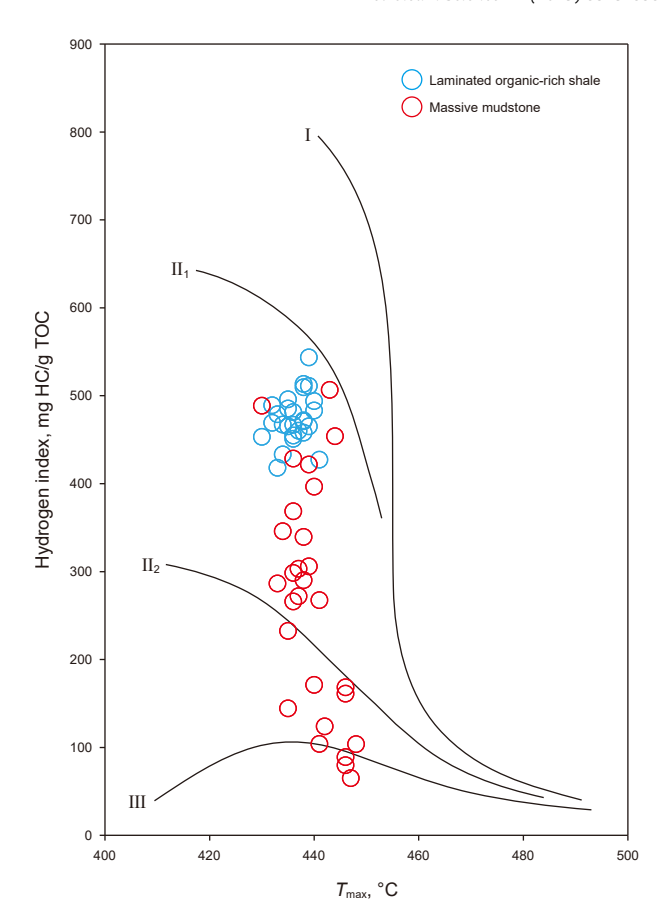


**Fig. 5.** Pyrolysis data for determining the kerogen type of the Mbr 7 of the Yanchang Fm in YYa borehole, showing that the kerogen type in the black shale samples is superior to that in the dark-gray mudstone samples.

LSC provides a direct approach to observing different occurrences of oil in shale. By analyzing variations in the color of fluorescence, various oil components, such as light and heavy oil, can be discerned (Hu et al., 2024). In general, shorter-wavelength fluorescence corresponds to lighter hydrocarbons, whereas longer-wavelength fluorescence indicates relatively heavier hydrocarbons (Liu et al., 2018). Typical LSC observations of the different lithofacies assemblages within Mbr 7 of the Yanchang Formation shale and mudstone are presented in Fig. 7. In laminated organic-rich shale samples, the intensity of shortwavelength fluorescence is subdued, indicating a low light oil concentration. Conversely, long-wavelength fluorescence is considerably more intense than short-wavelength fluorescence (Fig. 7(a) and (b)). Contrarily, massive mudstone samples exhibit a higher proportion of light oil compared with heavy oil (Fig. 7(d) and (e)). Despite the higher light oil content in the massive mudstone, the overall oil content within the laminated organicrich shale is greater owing to the higher heavy oil concentration (Fig. 7(c) and (f)).

### 5. Discussion

# 5.1. Differences in the formation mechanism of laminated organic-rich shale and massive mudstone

As previously discussed, the two lithofacies assemblages demonstrate notable differences in mineral composition, sedimentary textures, TOC content, and kerogen types, which reflect

**Table 1**Geochemical features of different lithofacies assemblages and sandstone interlayers of the Mbr 7 of the Yanchang Fm in YYa borehole.

Lithofacies assemblages	Lithofacies	TOC, wt%	S <sub>1</sub> , mg HC/g rock	S <sub>2</sub> , mg HC/g rock	S <sub>1</sub> +S <sub>2</sub> , mg HC/g rock	HI, mg HC/g TOC	OSI, mg HC/g TOC	TI	Sample amount
Laminated organic- rich shale	LRM	5.27–25.25 (13.93)	1.90–7.68 (4.87)	25.03–117.22 (65.98)	27.89–122.98 (70.85)	417.9–543.5 (476.0)	20.9–58.6 (36.9)	32.5–62.5 (50.8)	24
	LRCM	5.87–12.35 (9.11)	1.92–5.28 (3.60)	25.43–56.83 (41.13)	27.35–62.11 (44.73)	433.2–460.2 (446.7)	32.9–42.8 (37.7)		2
Gravity flow (hyperpycnal flow) sandstone	-	0.82–2.99 (1.93)	0.34–5.84 (3.13)	188–16.59 (9.50)	2.85–22.43 (12.63)	229.3–566.3 (464.8)	30.4–203.3 (148.6)	-	9
Massive mudstone	MRM	5.07	2.22	25.68	27.9	506.51	43.79	-53.9-45 (-9.5)	1
	MLM	0.77–4.57 (1.78)	0.17–3.02 (1.18)	0.50–19.27 (5.84)	0.67–21.40 (7.02)	64.9–488.6 (293.3)	21.3–215.7 (68.6)	, ,	12
	MLCM	0.73–3.17 (1.61)	0.09–1.47 (0.47)	0.65–12.57 (4.23)	0.75–13.83 (4.71)	89.1–396.5 (218.0)	48.98–322.63 (24.8)		13
	MLS	1.11–2.24 (1.68)	0.27–1.88 (1.08)	1.87–10.17 (6.02)	2.14–12.05 (7.10)	168.5–454.0 (311.2)	24.3–83.9 (54.1)		2
Delta front sandstone	-	0.25–2.82 (1.12)	0.06–8.16 (1.87)	0.25–17.51 (3.97)	0.43–22.66 (5.84)	73.8–620.9 (247.5)	9.8–356.2 (123.2)	-	13

Note: Minimum-maximum (average).

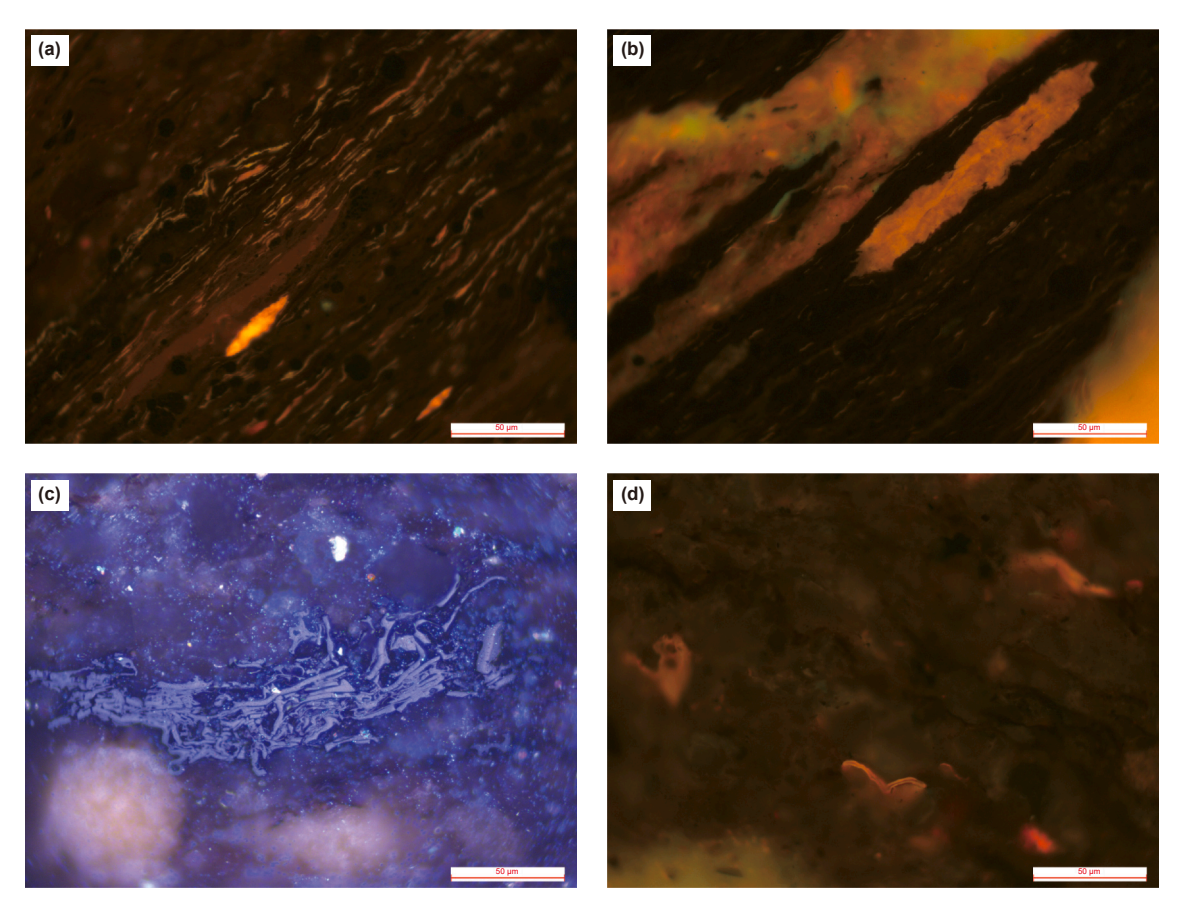


**Fig. 6.** Organic petrographic features for determining the kerogen type of the Mbr 7 of the Yanchang Formation in YYa borehole. ( $\mathbf{a}$ - $\mathbf{b}$ ) 229.51 m, black shale, TI = 62.5, indicating that the kerogen has relatively strong hydrocarbon generation potential; ( $\mathbf{c}$ - $\mathbf{d}$ ) 252.89 m, dark-gray mudstone, TI = -53.9, showing weaker hydrocarbon generation potential compared to the black shale sample. Fig. ( $\mathbf{a}$ ), ( $\mathbf{b}$ ), and ( $\mathbf{d}$ ) were taken under fluorescence illumination.

distinct depositional environments. As regards the mineral composition, the laminated organic-rich shale exhibit significantly lower levels of clay and quartz/feldspar than those found in massive mudstone. Previous studies have demonstrated that clay and quartz/feldspar can originate from terrigenous debris influx (Nichols, 2013; Katz and Lin, 2014; Khan et al., 2023; Wang et al., 2023a; Feng et al., 2023a; Yan et al., 2024). Thus, the mineralogical differences between laminated organic-rich shale and massive

mudstone imply variations in the quantity of terrigenous debris influx during deposition. The deposition phase of massive mudstone witnessed an increased influx of terrigenous debris, resulting in higher clay and quartz/feldspar contents.

Furthermore, the notable pyrite content in the laminated organic-rich shale warrants attention. Previous research has identified abundant framboidal pyrite with consistent grain sizes in the organic-rich shale of Mbr 7 of the Yanchang Formation in the

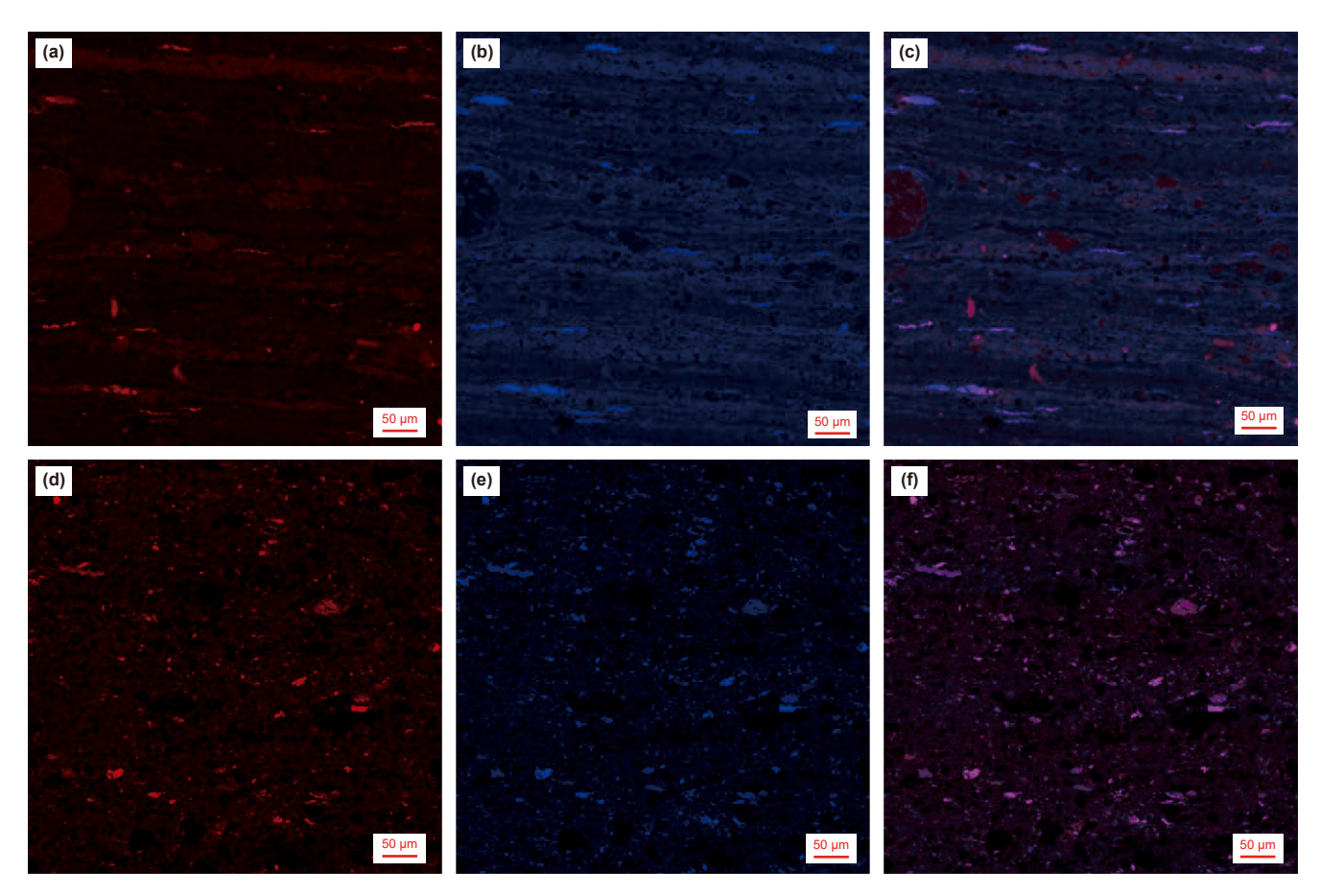


Fig. 7. Typical laser scanning confocal microscopy of the Mbr 7 of the Yanchang Fm. (a-c) 223.65 m, black shale, with a lower proportion of light hydrocarbons, predominantly consisting of heavy hydrocarbons; (d-f) 209.96 m, dark-gray mudstone, with a significantly lower heavy oil content compared to the sample of the black shale.

Ordos Basin (Wang et al., 2023c). Such a framboidal pyrite is typically considered to be contemporaneously formed during deposition, indicating an anoxic environment during that period (Bond and Wignall, 2010; Martínez-Yáñez et al., 2017). Thus, the elevated pyrite levels in the laminated organic-rich shale of Mbr 7 of the Yanchang Formation suggest prevailing anoxic conditions during deposition, a conclusion that is consistent with the reduced terrigenous debris content observed in the laminated organic-rich shale.

The variations in sedimentary textures further elucidate differences in depositional sedimentation rate. The transition from massive to laminated textures denotes an intensification in sedimentation rate during the sedimentation process (Potter et al., 1980; O'Brien and Slatt, 1990; Jin et al., 2023). Within Mbr 7 of the Yanchang Formation, laminated organic-rich shale are predominantly characterized by laminated textures, whereas those within massive mudstone mainly display massive textures. This implies that the massive mudstone were deposited under more faster sedimentation rate compared with their laminated organic-rich shale counterparts, thus corroborating the findings derived from mineral composition analyses.

Differences in depositional environments result in distinct geochemical characteristics (Tyson and Pearson, 1991; Algeo and Liu, 2020; Wu et al., 2021). The TOC content in the laminated organic-rich shale and massive mudstone within Mbr 7 of the Yanchang Formation exhibits considerable divergence. As previously discussed, the formation of abundant framboidal pyrite, indicating an anoxic depositional setting, created favorable conditions for organic matter preservation, which led to a strong

positive correlation between pyrite and TOC content (Fig. 8). Contrarily, the substantial influx of terrigenous debris during the deposition of massive mudstone likely diluted primary productivity, leading to a negative correlation between clay and quartz/ feldspar mineral content vs. TOC content (Fig. 8). Notably, while some researchers have suggested that increased terrigenous debris influx can enhance primary productivity (Algeo et al., 2001; Hartkopf-Fröder et al., 2007), Chen et al. (2021) also proposed that for Mbr 7 of the Yanchang Formation, increased terrigenous debris influx contributed to nutrient input from volcanic ash and subsequently boosted primary productivity. However, other studies on Mbr 7 of the Yanchang Formation have reported that heightened terrigenous debris influx and sedimentation rate can dilute organic matter (Chen et al., 2019). Out data clearly suggest that high terrigenous debris influx and sedimentation rate have had a negative effect on organic matter accumulation in Mbr 7 of the Yanchang Formation.

Moreover, the organic matter enrichment is influenced by primary productivity (Feng et al., 2023b). Previous studies have demonstrated that volcanic and hydrothermal activities such as volcanic fertilization (Duggen et al., 2007; Jones and Gislason, 2008; Zhang et al., 2017), have contributed to increased primary productivity, which led to organic matter enrichment. The integration of pyrolysis data with organic petrography observations provides a deeper understanding of the mechanisms driving organic matter enrichment. The pyrolysis results indicate that the HI values in the laminated organic-rich shale are considerably higher than those in massive mudstone, indicating greater hydrocarbon generation potential and superior kerogen types in

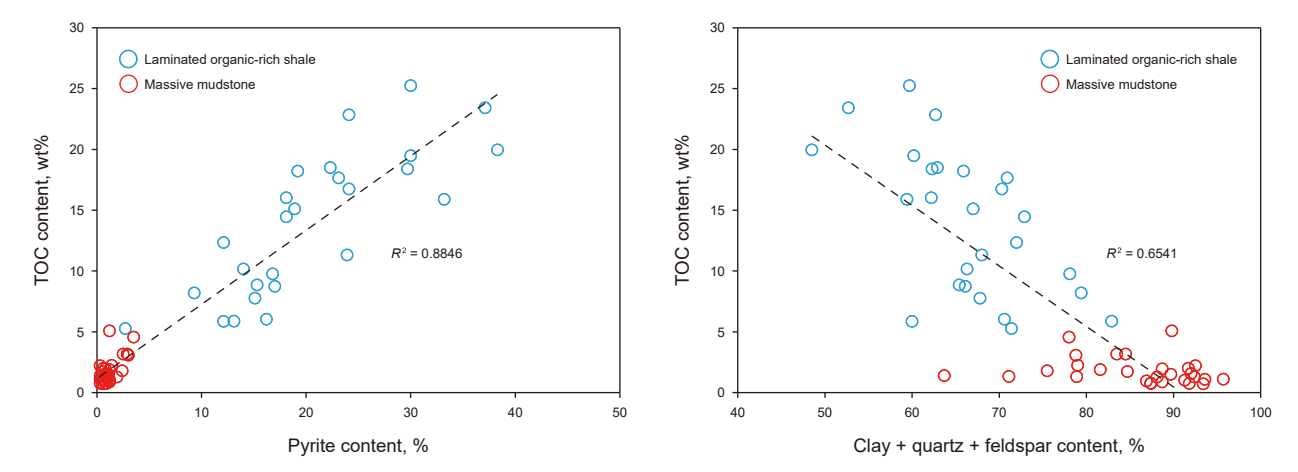


**Fig. 8.** The scatter plot indicates a strong positive correlation between TOC content and pyrite content, as well as a strong negative correlation between TOC content and clay + quartz + feldspar content in the laminated organic-rich shale and massive mudstone of Mbr 7 of the Yanchang Fm.

laminated organic-rich shale (Chen and Jiang, 2015). Moreover, organic petrographic analysis reveals a higher alginate content and a greater TI value in the laminated organic-rich shale. This observation further emphasizes the substantial contribution of aquatic organisms (*Leiosphaeridia* and *Botryococcus*, Zhang et al., 2015) to organic matter accumulation.

The variations in organic matter content among the lithofacies assemblages in Mbr 7 of the Yanchang Formation are influenced by the redox conditions and primary productivity during deposition. The oxygen-depleted environment and increased primary productivity during the formation of laminated organic-rich shale contributed to higher TOC content and formation of high-quality kerogen types.

Beyond the geological characteristics of laminated organic-rich shale and massive mudstone, the scale of sandstone interlayers also indicates the distinctions in depositional environments between the two lithofacies assemblages. There is a notable contrast in the thickness of sandstone layers within these assemblages (Fig. 2). In Mbr 7 of the Yanchang Formation of the YYa borehole, sandstone interlayers associated with laminated organic-rich shale generally have a thickness of less than 5 m, whereas those adjacent to massive mudstone are substantially thicker. This disparity is mainly attributed to the genesis of these sandstone interlayers. The sandstones within laminated organic-rich shale are usually formed by gravity-driven (hyperpycnal) flows (Zhao et al., 2020a; Jin et al., 2022), and commonly display normal grading characteristics.

The depositional environments of the various lithofacies assemblages in the Mbr 7 of the Yanchang Formation exhibit considerable differences. The deposition of laminated organic-rich shale occurred in relatively greater paleodepths, characterized by an anoxic environment with limited terrigenous debris influx and slow sedimentation rate. This facilitated the accumulation of pyrite and formation of a laminated texture. In addition, volcanic and hydrothermal activities substantially enhanced primary productivity (Ji et al., 2021; You et al., 2021; Liu et al., 2024), contributing to the formation of type II<sub>1</sub> kerogen and high TOC content. Conversely, during the deposition of massive mudstone, higher sedimentation rate and increased terrigenous debris influx led to higher clay and quartz/feldspar contents and massive texture. Furthermore, the amplified influx of terrigenous material diluted primary productivity, resulting in generally reduced TOC content and predominantly types II2 to III kerogen in the massive mudstone.

5.2. Identification of favorable exploration lithofacies assemblage in the Yanchang Formation

Oil content serves as the most direct indicator of resource potential. In laminated organic-rich shale, the S<sub>1</sub> values of LRM and LRCM are substantially higher than those of MRM, MLM, MLCM, and MLS in massive mudstone. This observation supports the notion that laminated organic-rich shale have a greater potential for hydrocarbon generation. However, in practical exploration, the physical state of the oil also plays a pivotal role in determining production outcomes (Wang et al., 2022). Specifically, free oil is more easily extracted than adsorbed oil (Jarvie, 2012; Pepper et al., 2019; Hu et al., 2021; Li et al., 2022b). Therefore, oil mobility should be carefully considered when assessing resource potential. Using the data from this study, we developed a model to illustrate the occurrence of oil in Mbr 7 of the Yanchang Formation (Fig. 9). Notably, organic matter acts as the primary carrier for sorption oil in shale (Li et al., 2016, 2022b). Hence, we employed the OSI proposed by Jarvie (2012) to represent the oil content per unit mass of TOC, accounting for variations in the TOC content across samples and reflecting oil mobility. Although the laminated organic-rich shale show greater overall oil content (Figs. 2 and 7), their OSI values are moderate owing to the high TOC content, indicating limited oil mobility—a finding consistent with the LSC observations. Conversely, while the oil content in massive mudstone is relatively modest, its OSI values are elevated, indicating improved oil mobility.

The differences in oil mobility between the two lithofacies assemblages can be attributed to several factors, including sedimentary texture, mineral composition, and geochemical characteristics. The laminated organic-rich shale mainly displays laminated textures, where organic matter and clay minerals often co-occur, with framework grains mainly suspended within the clay matrix (Fig. 3(c) and (e)). The plasticity of the organic matter and clay minerals, combined with the effects of compaction, impedes the formation of a rigid framework, thereby limiting the available space for free oil. Alternatively, the massive mudstone lithofacies, characterized by a substantial influx of terrigenous materials, introduce abundant quartz/feldspar that can interact under high-sedimentation rate conditions (Fig. 3(a)). This interaction creates a framework that partially resists compaction, thereby preserving the storage capacity for free oil.

From a geochemical perspective, laminated organic-rich shale is characterized by a notable TOC content and superior kerogen

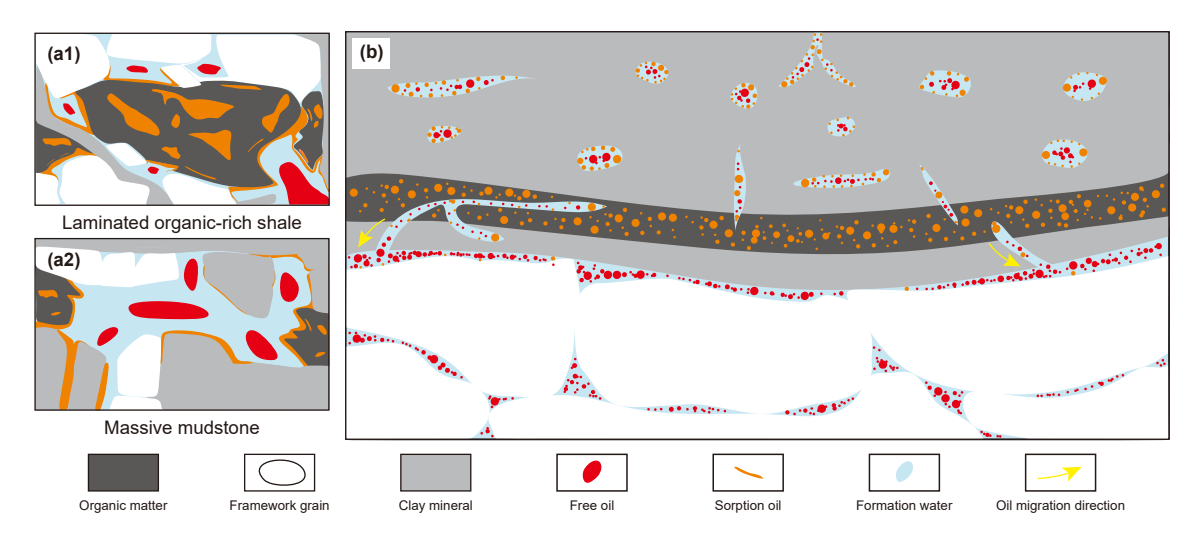


**Fig. 9.** Oil occurrence and migration models of the Mbr 7 of the Yanchang Fm. (a1) Oil occurrence model in the laminated organic-rich shale: A small amount of free oil resides in the pores of the shale, while a large amount of oil is present in a sorption state within the organic matter; (a2) Oil occurrence model in the massive mudstone: A small amount of free oil resides in the pores of the mudstone, but the low TOC abundance results in a relatively low content of sorbed oil; (b) Oil migration model of the laminated organic-rich shale (massive mudstone) and sandstone interlayers in the Mbr 7 of the Yanchang Fm, free oil is primarily found within the sandstone interlayers.

types. These favorable kerogen types are associated with a strong potential for hydrocarbon generation. However, the limited space for free oil within laminated organic-rich shale leads to the expulsion of a substantial amount of light oil, which has higher mobility. Consequently, heavier oil remains mainly in an adsorbed state within the organic matter. Despite the elevated oil content in the laminated organic-rich shale, the mobility of oil in these sedimentary rocks is constrained.

Contrarily, massive mudstone, with its relatively lower TOC content and less favorable kerogen types, experiences less considerable adsorption of oil by organic matter. Consequently, free oil can more readily occupy the shale pores. Although the overall oil content in the massive mudstone may not be as high, their oil mobility is more pronounced, thereby enhancing their exploration potential.

Assessment of exploration potential in laminated organic-rich shale and massive mudstone within Mbr 7 of the Yanchang Formation has already been conducted. This section mainly aims to shift the focus toward examination of the exploration potential of interlayer-type reservoirs within these lithofacies assemblages.

Mbr 7 of the Yanchang Formation is characterized by welldeveloped sandstone interlayers. Although the individual sandstone layers are relatively thin, the average ratio of sandstone to strata thickness is approximately 20%, which establishes a solid framework for hydrocarbon migration (Fu et al., 2021). Fu et al. (2021) reported that the oil saturation of sandstones in Mbr 7 of the Yanchang Formation can reach up to 90%, providing indirect support for the migration of hydrocarbons from laminated organic-rich shale (or massive mudstone) to adjacent sandstone interlayers. As regards the oil content, the S<sub>1</sub> values in sandstone interlayers do not markedly exceed those in clay-rich reservoirs. Notably, the S<sub>1</sub> values in the sandstone interlayers within laminated organic-rich shale are lower than those in LRM and LRCM. However, the oil mobility in sandstone interlayers is considerably superior to that in clay-rich reservoirs. This indicates that oil in clay-rich reservoirs with high TOC content mainly exists in an adsorbed state, which is consistent with the LSC observations, whereas the sandstone interlayers predominantly contain oil in a free state. Moreover, a comparison of oil content and mobility between sandstone interlayers formed by different depositional mechanisms shows that the S<sub>1</sub> and OSI values in sandstone

interlayers formed by gravity (hyperpycnal) flow surpass those in delta front sandstone interlayers, indicating superior oil content and mobility. This difference arises from the varying hydrocarbon generation capacities of the two lithofacies assemblages. Typically, gravity (hyperpycnal) flow sandstones develop within laminated organic-rich shale, where the clay-rich reservoir possess a substantially capacity for hydrocarbon generation but offer limited space for free oil storage. Consequently, much of the generated free oil undergoes primary migration into adjacent sandstone interlayers, leading to a more concentrated presence of oil within these sandstones. In addition, because the TOC content in these sandstones is relatively modest, the sorption effect of organic matter on oil is minimal, thereby enabling better oil mobility within these sandstone reservoirs. Although delta front sandstones share similar genesis mechanism to gravity (hyperpycnal) flow sandstones, the difference in geochemical characteristics between these two types of sandstone interlayers mainly arises from the distinct hydrocarbon generation potential and free oil storage capacity of the adjacent clay-rich reservoirs.

Based on the preceding discussion, we developed a theoretical model for oil occurrence in Mbr 7 of the Yanchang Formation reservoir (Fig. 9). The laminated organic-rich shales exhibit robust hydrocarbon generation potential, accounting for their relatively substantial oil content. However, the elevated TOC content causes significant oil sorption by organic matter, resulting in reduced oil mobility. Contrarily, the massive mudstone exhibits a more modest hydrocarbon generation potential, resulting in a comparatively lower oil content than that in laminated organic-rich shale. Nevertheless, the reduced TOC content in the massive mudstone means that oil adsorption by organic matter is less pronounced. In addition, the mineralogical composition and sedimentary textures of the massive mudstone provide additional space for the accumulation of free oil, thereby enhancing oil mobility compared with the laminated organic-rich shale.

As regards the sandstone interlayers formed by different depositional mechanisms, the mechanism of hydrocarbon charging is similar, with free oil generated in the adjacent clay-rich reservoirs migrating mainly into these sandstones. The variations in their geochemical characteristics are largely determined by the hydrocarbon generation capacity of the adjacent shales and mudstones and the impact of oil sorption. It is essential to

highlight that the sandstone interlayers within laminated organic-rich shale deposited by the gravity (hyperpycnal) flow should be prioritized as primary exploration targets in Mbr 7 of the Yanchang Formation due to their superior oil mobility. Following these, the delta front sandstones within massive mudstone should be considered. Among the clay-rich reservoir, those in massive mudstone exhibit greater oil mobility than those in laminated organic-rich shale, indicating a higher exploration potential considering the current technological capabilities.

# 5.3. Preconditions of clay-rich reservoirs can serve as effective exploration targets in lacustrine shale systems

Previous studies have demonstrated that in lacustrine shale systems deposited under predominantly freshwater conditions, favorable exploration targets are mainly interlayer-type shale oil reservoirs. For example, Wang et al. (2023b) highlighted the importance of considering sandstone and carbonate interlayers in lacustrine shale systems that form under predominantly freshwater conditions. Similarly, Guo et al. (2023) suggested that in predominantly freshwater environments, there is often a separation between source rocks and reservoirs, with interlayers within the shale system potentially holding a greater exploration value. The findings of this study are consistent with the previous conclusions. However, not all clay-rich reservoirs in lacustrine shale systems formed under predominantly freshwater conditions are difficult to explore (Guo et al., 2023). For example, significant exploration breakthroughs have been achieved in the clay-rich reservoirs of the Cretaceous Oingshankou Formation in the Songliao Basin (Sun et al., 2023). This raises a critical question: Why do exploration outcomes for clay-rich reservoirs greatly differ within lacustrine shale systems deposited in predominantly freshwater conditions? This study seeks to address this question by comparing Mbr 7 of the Yanchang Formation of the Ordos Basin and Cretaceous Qingshankou Formation of the Songliao Basin, to elucidate the conditions under which clay-rich reservoirs in lacustrine shale systems deposited in predominantly freshwater environments hold exploration value.

The geochemical characteristics of the clay-rich shale reservoirs in two lacustrine shale systems are presented in detail in Table 2. To distinguish the differences in exploration potential among these shale systems, it is imperative to examine oil content and mobility. Remarkably, the oil content of the clay-rich reservoirs of the Cretaceous Qingshankou Formation is significantly higher than that in Mbr 7 of the Yanchang Formation. This finding may initially appear counterintuitive, as the TOC content is typically considered to be the primary determinant of oil content in lacustrine shale systems. Despite the higher TOC content in the clay-rich reservoirs of Mbr 7 of the Yanchang Formation compared with those of the Cretaceous Qingshankou Formation, its oil content is lower. This discrepancy suggests the presence of additional factors influencing oil content. In terms of hydrocarbon generation capacity (kerogen type), the clay-rich reservoirs of Mbr 7 of the Yanchang Formation and the Cretaceous Qingshankou Formation are similar. Therefore, the disparity in oil content between Mbr 7 of the Yanchang Formation and the Cretaceous Qingshankou Formation is most likely attributable to differences in petroleum migration. Preservation conditions are known to play a pivotal role in the determination of oil content in shale reservoirs (Guo et al., 2023). As aforementioned, the pores of the clay-rich reservoirs in Mbr 7 of the Yanchang Formation were often not preserved during diagenesis, with the majority of generated light oil migrating into adjacent sandstone interlayers. This resulted in the clay-rich reservoirs of Mbr 7 of the Yanchang Formation being in a normal pressure state (pressure coefficient, approximately 0.9-1.2; Gu

et al., 2021), thereby contributing to its relatively modest oil content. Meanwhile, studies on the Cretaceous Qingshankou Formation indicate that it mainly comprises thick shale succession with minimal development of sandstone interlayers (Liu et al., 2022; Wu et al., 2023). The preservation conditions of these shale reservoirs are excellent, characterized by significant pressure anomalies (pressure coefficients, 1.0-1.2) and regions of overpressure (pressure coefficients, >1.2). Therefore, extensive petroleum migration has not occurred within the clay-rich reservoirs of the Cretaceous Qingshankou Formation. Moreover, owing to the high thermal maturity of the Cretaceous Qingshankou Formation (Zhao et al., 2020a), diagenetic processes such as clay mineral transformation, mineral dissolution, and organic matter pore development have led to the formation of a well-developed pore system (Liu et al., 2018; Sun et al., 2023). These pores provide ample storage capacity for hydrocarbons, enabling substantial quantities of petroleum to remain within the shale. Experimental simulations conducted by Sun et al. (2023) on hydrocarbon generation, expulsion, and retention in the shale of the Cretaceous Qingshankou Formation exhibited an oil expulsion efficiency of ~20%, supporting our analysis.

In addition, the oil mobility in the Cretaceous Qingshankou Formation is higher than that in Mbr 7 of the Yanchang Formation. The variation in oil mobility could be mainly attributed to differences in thermal maturity and preservation conditions. Increased thermal maturity causes substantial changes in oil mobility. It promotes the cracking of heavier hydrocarbons into lighter fractions, resulting in a higher gas-oil ratio (GOR) and improved oil mobility (Wang et al., 2024a). Furthermore, the structural changes in kerogen resulting from hydrocarbon generation decrease the sorption capacity of organic matter to oil as thermal maturity progresses (Wei et al., 2012; Pepper et al., 2019; Li et al., 2022b; Wang et al., 2022; Pan et al., 2023). Consequently, the clay-rich reservoirs of the Cretaceous Qingshankou Formation are characterized by enhanced oil mobility. Additionally, the Cretaceous Qingshankou Formation exhibits limited sandstone development, leading to a low sandstone-strata thickness ratio and a predominantly closed preservation system. In this context, despite the substantial TOC content in the shale of the Cretaceous Qingshankou Formation, it still exhibits the most efficient oil mobility. Meanwhile, in the clay-rich reservoirs of Mbr 7 of the Yanchang Formation, particularly in Basin margin areas with lower thermal maturity, the strong adsorption of oil by organic matter restricts oil mobility. In regions where thermal maturity reaches the middle oil window, the sandstone-strata thickness ratio, which is a critical indicator of preservation conditions, determines whether hydrocarbons remain primarily in situ or migrate into adjacent sandstone interlayers. Thus, for clay-rich reservoirs, increased thermal maturity, abundant organic matter, and optimal preservation conditions are crucial prerequisites for a successful exploration.

The comparison of the clay-rich reservoirs of Mbr 7 of the Yanchang Formation and Cretaceous Qingshankou Formation reveals that clay-rich reservoirs deposited under the predominantly-freshwater condition generally present substantial challenges for exploration and development. As such, the focus should be on targeting interlayer-type reservoirs as the primary exploration and development targets at present. For clay-rich reservoirs, achieving considerable breakthroughs require a combination of advanced thermal maturity, high organic matter content, and the presence of great preservation condition, which together improve the exploration potential. Based on this rationale, the clay-rich reservoirs of Mbr 7 of the Yanchang Formation, which is located in the central Ordos Basin (e.g., the Huachi and Wuqi areas), may hold promising exploration potential. On the one hand, the shales in these depositional centers exhibit higher thermal maturity ( $R_0$  more than

reservoirs in the Mbr 7 of the Triassic Yanchang Formation in the Ordos Basin and Cretaceous Oingshankou Formation in the Songliao Basin. Comparison of geological characteristics of the clay-rich shale

Strata	Mineral composition	TOC content, wt%	Kerogen type	Thermal maturity	S <sub>1</sub> , mg HC/g rock	Pressure coefficient	Oil mobility	Influence mechanisms of the petroleum production	References
Cretaceous Qingshankou Formation	Clay mineral dominates the mineral composition	2.0-6.0 (3.8)	FII <sub>1</sub>	R <sub>0</sub> ranges from 0.8 to 1.7%, with most values greater than 1.2%.	4.0–15.0	The high pressure anomaly (1.0–1.2) and overpressure (>1.2) are generally existed	OSI is greater than 200 mg HC/g TOC, and the GOR is generally above 200 m³/m³	The relatively high TOC content and superior kerogen type provide a solid material basis for hydrocarbon accumulation. Additionally, the high thermal maturity results in high oil mobility, thereby forming perroleum sweet snots.	Liu et al. (2018); Zhao et al. (2020b); Li et al. (2022a); Ma et al. (2022); Guo et al. (2023)
Mbr 7 of the Triassic Yanchang Formation	Clay mineral dominates the mineral composition with high content of pyrite	0.7–25.3 (7.7)	<u>-</u>	Average R <sub>o</sub> is 0.71%	0.1–7.7 (2.8)	0.9–1.2	OSI ranges from 12 to 215 mg HC/g TOC, with an average value of 42 mg HC/g TOC.	The high TOC content and superior kerogen type confer a high hydrocarbon generation potential. However, the excessive TOC results in oil being primarily adsorbed in laminated organic-rich shale, with most of the free oil already migrated. Therefore, it cannot currently be considered a primary exploration target.	This study: Guetal. (2021)

1.0%), thereby providing a foundation for the development of organic pores and improved oil mobility. In addition, these centers are more conducive to the formation of laminated organic-rich shale, with lower sandstone–strata thickness ratios, which supports oil retention and preservation.

#### 6. Conclusions

This study centers on Mbr 7 of the Yanchang Formation in the Tongchuan region of the southern Ordos Basin. The main objective is to systematically assess the exploration potential of different lithofacies assemblages. Additionally, we discuss the conditions under which clay-rich shale reservoirs formed in predominantly freshwater environments may serve as favorable exploration targets. The principal findings are as follows:

The laminated organic-rich shale was deposited within an anoxic setting characterized by increased primary productivity, whereas the massive mudstone originated in an environment with a higher sedimentation rate and increased terrigenous influx. These contrasting environmental conditions have led to notable geological variations between the two lithofacies assemblages.

Despite the relatively high oil content in the clay-rich reservoirs of Mbr 7 of the Yanchang Formation, the mobility of oil is markedly limited owing to primary hydrocarbon migration. Considering the current technological capabilities, sandstone interlayers exhibit notably greater exploration potential than shales and mudstones. Specifically, the sandstone interlayers within laminated organic-rich shale, deposited by gravity (hyperpycnal) flow, present the most promising prospects. Within the category of clay-rich reservoirs, massive mudstone exhibits higher exploration potential.

The clay-rich reservoirs present in lacustrine shale systems, formed mainly under freshwater conditions, often present considerable challenges for exploration and development. Consequently, it is advisable to prioritize interlayer-type reservoirs in ongoing exploration and development endeavors. However, in situations where there is advanced thermal maturity, abundant organic matter, and favorable preservation conditions, clay-rich reservoirs within lacustrine shale systems may also provide valuable exploration opportunities.

#### **CRediT authorship contribution statement**

Enze Wang: Writing – original draft, Investigation. Maowen Li: Writing – original draft, Funding acquisition, Conceptualization. Xiaoxiao Ma: Resources. Menhui Qian: Data curation, Resources. Tingting Cao: Data curation, Resources. Zhiming Li: Data curation, Resources. Sen Li: Resources. Zhijun Jin: Project administration, supervision.

#### **Declaration of competing interest**

The authors declare that they have no known competing financial interests or personal relationships that could have appeared to influence the work reported in this paper.

#### Acknowledgments

This study is supported by the National Natural Science Foundation of China (Projects 42090022).

#### References

Abouelresh, M.O., Slatt, R.M., 2012. Lithofacies and sequence stratigraphy of the barnett shale in east-central Fort Worth Basin, Texas. AAPG (Am. Assoc. Pet. Geol.) Bull. 96 (1), 1–22. https://doi.org/10.1306/04261110116.

Note: Minimum-maximum (average)

Algeo, T.J., Liu, J.S., 2020. A re-assessment of elemental proxies for paleoredox analysis. Chem. Geol. 540, 119549. https://doi.org/10.1016/j.chemgeo.2020.

- Algeo, T.J., Scheckler, S.E., Maynard, J.B., 2001. Effects of the middle to late Devonian spread of vascular land plants on weathering regimes, marine biotas, and global climate. In: Gensel, P.G., Edwards, D. (Eds.), Plant Invade the Land: Evolutionary and Environmental Perspectives, pp. 213–236. https://doi.org/10.7312/gens11160.
- Bohacs, K.M., Carroll, A.R., Neal, J.E., Mankiewicz, P.J., 2000. Lake-Basin type, source potential, and hydrocarbon character: an integrated sequence-stratigraphic-geochemical framework. In: Gierlowski-Kordesch, E.H., Kelts, K.R. (Eds.), Lake basins Through Space and Time, pp. 3–34. https://doi.org/10.1306/St46706.
- Bond, D.P.G., Wignall, P.B., 2010. Pyrite framboid study of marine Permian-Triassic boundary sections: a complex anoxic event and its relationship to contemporaneous mass extinction. Geol. Soc. Am. Bull. 122 (7–8), 1265–1279. https:// doi.org/10.1130/B30042.1.
- Cao, H.R., Shi, J., Zhan, Z.W., Wu, H., Wang, X.Y., Cheng, X., Li, H.L., Zou, Y.R., Peng, P. A., 2024. Shale oil potential and mobility in low- to medium-maturity lacustrine shales: A case study of the Yanchang Formation shale in southeast Ordos Basin, China. Int. J. Coal Geol. 282, 104421. https://doi.org/10.1016/j.coal.2023.104421
- Chen, Z.H., Guo, Q.L., Jiang, C.Q., Liu, X.J., Reyes, J., Mort, A., Jia, Z.K., 2017. Source rock characteristics and Rock-Eval-based hydrocarbon generation kinetic models of the lacustrine Chang-7 Shale of Triassic Yanchang Formation, Ordos Basin, China. Int. J. Coal. Geol. 182, 52–65. https://doi.org/10.1016/j.coal.2017.08.017
- Chen, Z., Jiang, C.Q., 2015. A data driven model for studying kerogen kinetics with application examples from Canadian sedimentary basins. Mar. Petrol. Geol. 67, 795–807. https://doi.org/10.1016/j.marpetgeo.2015.07.004.
- Chen, G., Gang, W.Z., Liu, Y.Z., Wang, N., Guo, Y., Zhu, C.Z., Cao, Q.Y., 2019. High-resolution sediment accumulation rate determined by cyclostratigraphy and its impact on the organic matter abundance of the hydrocarbon source rock in the Yanchang Formation, Ordos Basin, China. Mar. Petrol. Geol. 103, 1–11. https://doi.org/10.1016/j.marpetgeo.2019.01.044.
- Chen, X.L., Zhang, B., Huang, H.P., Mao, Z.G., 2021. Controls on organic matter accumulation of the Triassic Yanchang Formation lacustrine shales in the Ordos Basin, North China. ACS Omega 6 (40), 26048–26064. https://doi.org/10.1021/acsomega.1c02993.
- Deng, S.H., Lu, Y.Z., Luo, Z., Fan, R., Li, X., Zhao, Y., Ma, X.Y., Zhu, R.K., Cui, J.W., 2018. Subdivision and age of the Yanchang Formation and the middle/upper Triassic boundary in Ordos Basin, North China. Sci. China Earth Sci. 61 (10), 1419–1439. https://doi.org/10.1007/s11430-017-9215-3.
- Duggen, S., Croot, P., Schacht, U., Hoffmann, L., 2007. Subduction zone volcanic dust can fertilize the surface ocean and stimulate phytoplankton growth: evidence from biogeochemical experiments and satellite data. Geophys. Res. Lett. 34, L01612. https://doi.org/10.1029/2006GL027522.
- EIA, 2024. How Much Shale (Tight) Oil Is Produced in the United States? https://www.eia.gov/tools/faqs/faq.php?id=847&t=6.
- Fan, X.J., Lu, Y.B., Liu, Z.H., Lu, Y.C., Zhang, J.Y., Deng, K., Zhou, T., Tai, H., Li, L., 2024. Lacustrine shale lithofacies and depositional environment in the Paleocene second member of the Funing Formation, Subei Basin, China: Insights into shale oil development prospects. Mar. Petrol. Geol. 164, 106849. https://doi. org/10.1016/j.marpetgeo.2024.106849.
- Feng, Y., Xiao, X.M., Gao, P., Wang, E.Z., Hu, D.F., Liu, R.B., Li, G., Lu, C.G., 2023a. Restoration of sedimentary environment and geochemical features of deep marine Longmaxi shale and its significance for shale gas: A case study of the Dingshan area in the Sichuan Basin, South China. Mar. Petrol. Geol. 151, 106186. https://doi.org/10.1016/j.marpetgeo.2023.106186.
- Feng, Y., Xiao, X.M., Wang, E.Z., Gao, P., Lu, C.G., Li, G., Wang, Z.H., Zhou, Q., 2023b. Origins of siliceous minerals and their influences on organic matter enrichment and reservoir physical properties of deep marine shale in the sichuan Basin, south China. Energy Fuels 37 (16), 11982–11995. https://doi.org/10.1021/acs.energyfuels.3c01702.
- Fu, J.H., Guo, W., Li, S.X., Liu, X.Y., Cheng, D.X., Zhou, X.P., 2021. Characteristics and exploration potential of muti-type shale oil in the 7th member of Yanchang Formation, Ordos Basin. Nat. Gas Geosci. 32 (12), 1749–1761. https://doi.org/ 10.11764/j.issn.1672-1926.2021.07.016 (in Chinese).
- Gamero-Diaz, H., Miller, C., Lewis, R.E., 2013. Score: A Mineralogy Based Classification Scheme for Organic Mudstones. SPE Annual Technical Conference, New Orleans, 40951 (SPE 166284). doi: http://doi.org/10.2118/166284-MS.
- Gu, Z.Y., Liu, E.T., Wang, X.Z., Li, R.X., Xu, J.S., Zhou, B., 2021. Development characteristics and exploration potential of shale in Chang7 member in southeast of Ordos Basin. Petroleum Geology and Recovery Efficiency 28 (1), 95–105. https://doi.org/10.13673/j.cnki.cn37-1359/te.2021.01.012 (in Chinese).
- Guo, X.S., Ma, X.X., Li, M.W., Qian, M.H., Hu, Z.Q., 2023. Mechanisms for lacustrine shale oil enrichment in Chinese sedimentary Basins. Oil Gas Geol 44 (6), 1333–1349. https://doi.org/10.11743/ogg20230601 (in Chinese).
- Han, C., Jiang, Z.X., Han, M., Wu, M.H., Lin, W., 2016. The lithofacies and reservoir characteristics of the Upper Ordovician and Lower Silurian Black shale in the southern sichuan Basin and its periphery, China. Mar. Petrol. Geol. 75, 181–191. https://doi.org/10.1016/j.marpetgeo.2016.04.014.
- Hartkopf-Fröder, C., Kloppisch, M., Mann, U., Neumann-Mahlkau, P., Schaefer, R.G., Wilkes, H., 2007. The end-Frasnian mass extinction in the Eifel Mountains, Germany: new insights from organic matter composition and preservation. In: Becker, R.T., Kirchgasser, W.T. (Eds.), Devonian Events and Correlations.

- Geological Society London, Special Publications 278, pp. 173–196. https://doi.org/10.1144/SP278.8
- He, X.B., Luo, Q., Jiang, Z.X., Qiu, Z.X., Luo, J.C., Li, Y.Y., Deng, Y., 2024. Control of complex lithofacies on the shale oil potential in saline lacustrine Basins of the Jimsar Sag, NW China: Coupling mechanisms and conceptual models. J. Asian Earth Sci. 266, 106135. https://doi.org/10.1016/j.jseaes.2024.106135.
- Hu, T., Pang, X.Q., Jiang, F.J., Wang, Q.F., Liu, X.H., Wang, Z., Jiang, S., Wu, G.Y., Li, C.J., Xu, T.W., Li, M.W., Yu, J.W., Zhang, C.X., 2021. Movable oil content evaluation of lacustrine organic-rich shales: Methods and a novel quantitative evaluation model. Earth Sci. Rev. 214, 103545. https://doi.org/10.1016/j.earscirev.2021. 103545.
- Hu, T., Wu, G.Y., Xu, Z., Pang, X.Q., Liu, Y., Yu, S., 2022. Potential resources of conventional, tight, and shale oil and gas from Paleogene Wenchang Formation source rocks in the Huizhou depression. Advances in Geo-Energy Research 6 (5), 402–414. https://doi.org/10.46690/ager.2022.05.05.
- Hu, T., Jiang, F.J., Pang, X.Q., Liu, Y., Wu, G.Y., Zhou, K., Xiao, H.Y., Jiang, Z.X., Li, M.W., Jiang, S., Huang, L.L., Chen, D.X., Meng, Q.Y., 2024. Identification and evaluation of shale oil micromigration and its petroleum geological significance. Petrol. Explor. Dev. 51 (1), 127–140. https://doi.org/10.1016/S1876-3804(24)60010-8.
- Hughes, J.D., 2013. A reality check on the shale revolution. Nature 494, 307–308. https://doi.org/10.1038/494307a.
- Iqbal, M.A., Rezaee, R., Smith, G., Ekundayo, J.M., 2021. Shale lithofacies controls on porosity and pore structure: an example from Ordovician Goldwyer Formation, Canning Basin, Western Australia. J. Nat. Gas Sci. Eng. 89, 103888. https://doi. org/10.1016/j.jngse.2021.103888.
- Jarvie, D.M., 2012. Shale resource systems for oil and gas: part 2-shale-oil resource systems. In: Breyer, J.A. (Ed.), Shale Reservoirs Giant Resources for the 21st Century, vol. 97. Am. Assoc. Petrol. Geol. Mem., pp. 89–119. https://doi.org/10. 1306/13321447M973489.
- Ji, L.M., Yan, K., Meng, F.W., Zhao, M., 2010. The oleaginous botryococcus from the Triassic Yanchang formation in Ordos Basin, Northwestern China: Morphology and its paleoenvironmental significance. J. Asian Earth Sci. 38, 175–185. https:// doi.org/10.1016/j.jseaes.2009.12.010.
- Ji, L.M., Li, J.F., Zhang, M.Z., Lu, H., He, C., Jin, P.H., Ma, B., 2021. Effects of lacustrine hydrothermal activity on the organic matter input of source rocks during the Yanchang period in the Ordos Basin. Mar. Petrol. Geol. 125, 104868. https://doi. org/10.1016/j.marpetgeo.2020.104868.
- Jin, Z.J., Yang, R.C., Loon, A.J.V., Han, Z.Z., Fan, A.P., 2022. The origin of hyperpycnites in the middle-late Triassic Yanchang fm. (Ordos Basin, China) and their significance for the formation of unconventional hydrocarbons. In: Yang, R.C., van Loon, A.J. (Eds.), The Ordos Basin: Sedimentological Research for Hydrocarbons Exploration, pp. 337–352. https://doi.org/10.1016/B978-0-323-85264-7.00001-1
- Jin, Z.J., Zhang, Q., Zhu, R.K., Dong, L., Fu, J.H., Liu, H.M., Yun, L., Liu, G.Y., Li, M.W., Zhao, X.Z., Wang, X.J., Hu, S.Y., Tang, Y., Bai, Z.R., Sun, D.S., Li, X.G., 2023. Classification of lacustrine shale oil reservoirs in China and its significance. Oil Gas Geol 44 (4), 801–819 (in Chinese). https://doi.org/10.11743/ogg20230401.
- Jones, M.T., Gislason, S.R., 2008. Rapid release of metal salts and nutrients following the deposition of volcanic ash into aqueous environments. Geochem. Cosmochim. Acta 72, 3661–3680. https://doi.org/10.1016/j.gca.2008.05.030.
- Kang, Z.Q., Zhao, Y.S., Yang, D., 2020. Review of oil shale in-situ conversion technology. Appl. Energy 269, 115121. https://doi.org/10.1016/j.apenergy.2020. 115121
- Katz, B., Lin, F., 2014. Lacustrine Basin unconventional resource plays: key differences. Mar. Petrol. Geol. 56, 255–265. https://doi.org/10.1016/j.marpetgeo. 2014.02.013.
- Khan, D., Liu, Z.J., Qiu, L.W., Liu, K.Y., Yang, Y.Q., Nie, C., Liu, B., Xin, L., Yerejiepu, H., 2023. Mineralogical and geochemical characterization of lacustrine calcareous shale in Dongying depression, Bohai Bay Basin: Implications for paleosalinity, paleoclimate, and paleoredox conditions. Geochemistry 83 (3), 125978. https://doi.org/10.1016/j.chemer.2023.125978.
- Lazar, O.R., Bohacs, K.M., Macquaker, J.H.S., Schieber, J., Demko, T.M., 2015. Capturing key attributes of fine-grained sedimentary rocks in outcrops, cores, and thin sections: Nomenclature and description guidelines. J. Sediment. Res. 83 (3/4), 230–246. https://doi.org/10.2110/jsr.2015.11.
- Li, Z., Zou, R.Y., Xu, X.Y., Sun, J.N., Li, M.W., Peng, P.A., 2016. Adsorption of mudstone source rock for shale oil experiments, model and a case study. Org. Geochem. 92, 55–62. https://doi.org/10.1016/j.orggeochem.2015.12.009.
- Li, J.R., Yang, Z., Wu, S.T., Pan, S.Q., 2021. Key issues and development direction of petroleum geology research on source rock strata in China. Advances in Geo-Energy Research 5 (2), 121–126. https://doi.org/10.46690/ager.2021.02.02.
- Li, M.W., Ma, X.X., Jin, Z.J., Li, Z.M., Jiang, Q.G., Wu, S.Q., Li, Z., Xu, Z.X., 2022a. Diversity in the lithofacies assemblages of marine and lacustrine shale strata and significance for unconventional petroleum exploration in China. Oil Gas Geol. 43 (1), 1–25. https://doi.org/10.11743/ogg20220101 (in Chinese).
- Li, J.B., Wang, M., Jiang, C.Q., Lu, S.F., Li, Z., 2022b. Sorption model of lacustrine shale oil: insights from the contribution of organic matter and clay minerals. Energy 260, 125011. https://doi.org/10.1016/j.energy.2022.125011.
- Liang, C., Cao, Y.C., Jiang, Z.X., Wu, J., Song, G.Q., Wang, Y.S., 2017. Shale oil potential of lacustrine Black shale in the Eocene Dongying depression: Implications for geochemistry and reservoir characteristics. AAPG (Am. Assoc. Pet. Geol.) Bull. 101 (11), 1835–1858. https://doi.org/10.1306/01251715249.
- Liu, B., Shi, J.X., Fu, X.F., Lyu, Y.F., Sun, X.D., Gong, L., Bai, Y.F., 2018. Petrological characteristics and shale oil enrichment of lacustrine fine-grained sedimentary system: A case study of organic-rich shale in first member of Cretaceous

Qingshankou Formation in Gulong sag, Songliao Basin, NE China. Petrol. Explor. Dev. 45 (5), 884–894. https://doi.org/10.1016/S1876-3804(18)30091-0.

- Liu, B., Wang, H.L., Fu, X.F., Bai, Y.F., Bai, L.H., Jia, M.C., He, B., 2019. Lithofacies and depositional setting of a highly prospective lacustrine shale oil succession from the Upper Cretaceous Qingshankou Formation in the Gulong sag, northern Songliao Basin, Northeast China. AAPG (Am. Assoc. Pet. Geol.) Bull. 103 (2), 405–432. https://doi.org/10.1306/08031817416.
   Liu, B., Nakhaei-Kohani, R., Bai, L.H., Wen, Z.G., Gao, Y.F., Tian, W.C., Yang, L., Liu, K.
- Liu, B., Nakhaei-Kohani, R., Bai, L.H., Wen, Z.G., Gao, Y.F., Tian, W.C., Yang, L., Liu, K. Q., Hemmati-Sarapardeh, A., Ostadhassan, M., 2022. Integrating advanced soft computing techniques with experimental studies for pore structure analysis of Qingshankou shale in southern Songliao Basin, NE China. Int. J. Coal Geol. 257, 103998. https://doi.org/10.1016/j.coal.2022.103998.
- Liu, Q.Y., Li, P., Jiang, L., Jin, Z.J., Liang, X.P., Zhu, D.Y., Pang, Q., Zhang, R., Liu, J.Y., 2024. Distinctive volcanic ash-rich lacustrine shale deposition related to chemical weathering intensity during the Late Triassic: Evidence from lithium contents and isotopes. Sci. Adv. 10 (11). https://doi.org/10.1126/sciadv.adi6594.
- Loucks, R.G., Ruppel, S.C., 2007. Mississippian barnett shale: Lithofacies and depositional setting of a deep-water shale-gas succession in the Fort Worth Basin, Texas. AAPG. Am. Assoc. Petrol. Geol. Bull. 91, 579–601. https://doi.org/10.1306/110.20606059.
- Ma, Y.S., Cai, X.Y., Zhao, P.R., Hu, Z.Q., Liu, H.M., Gao, B., Wang, W.Q., Li, Z.M., Zhang, Z.L., 2022. Geological characteristics and exploration practices of Continental shale oil in China. Acta Geol. Sin. 96 (1), 155–171 (in Chinese). https://doi.org/10.19762/j.cnki.dizhixuebao.2022278.
- Martínez-Yáñez, M., Núñez-Useche, F., López Martínez, R., Gardner, R.D., 2017. Paleoenvironmental conditions across the Jurassic-Cretaceous boundary in central-eastern Mexico. J South Am Earth Sci. 77, 261–275. https://doi.org/10. 1016/i.isames.2017.05.007.
- Nichols, G., 2013. Sedimentology and Stratigraphy. second ed. Wiley-Blackwell, Chichester, UK; Hoboken, NJ. https://www.wiley.com/en-mx/Sedimentology+and+Stratigraphy%2C+2nd+Edition-p-9781118687772
- O'Brien, N.R., Slatt, R.M., 1990. Argillaceous Rock Atlas. Springer-Verlag, New York. https://doi.org/10.1007/978-1-4612-3422-7.
- Pan, Y.H., Li, M.W., Sun, Y.C., Li, Z.M., Liao, L.L., Liao, Y.H., 2023. Characterization of free and bound bitumen fractions in a thermal maturation shale sequence. Part 2: Structural evolution of kerogen and bitumen during shale oil generation, expulsion and retention. Org. Geochem. 182, 104640. https://doi.org/10.1016/j. orggeochem.2023.104640.
- Pepper, A., Perry, S., Heister, L., 2019. Saturation isn't what it used to be: Towards more realistic petroleum fluid saturations and produced fluid compositions in organic-rich unconventional reservoirs. In: Unconventional Resources Technology Conference. https://doi.org/10.15530/urtec-2019-196.
- Potter, P.E., Maynard, J.B., Pryor, W.A., 1980. Sedimentology of shale: Study guide and reference source. Springer-Verlag, New York. https://doi.org/10.1007/978-1.4613.0081.2
- Qiao, J.Q., Baniasad, A., Zieger, L., Zhang, C., Luo, Q., Littke, R., 2021. Paleo-depositional environment, origin and characteristics of organic matter of the Triassic Chang 7 member of the Yanchang Formation throughout the mid-western part of the Ordos Basin, China. Int. J. Coal Geol. 237, 103636. https://doi.org/10.1016/j.coal.2020.103636.
- Sun, L.D., Liu, H., He, W.Y., Li, G.X., Zhang, S.C., Zhu, R.K., Jin, X., Meng, S.W., Jiang, H., 2021. An analysis of major scientific problems and research paths of Gulong shale oil in Daqing oilfield, NE China. Petrol. Explor. Dev. 48 (3), 527–540. https://doi.org/10.1016/S1876-3804(23)60406-9.
- Sun, L.D., Cui, B.W., Zhu, R.K., Wang, R., Feng, Z.H., Li, B.H., Zhang, J.Y., Gao, B., Wang, Q.Z., Zeng, H.S., Liao, Y.H., Jiang, H., 2023. Shale oil enrichment evaluation and production law in Gulong Sag, Songliao Basin, NE China. Petrol. Explor. Dev. 50 (3), 505–519. https://doi.org/10.1016/S1876-3804(23)60406-9.
- Tyson, R.V., Pearson, T.H., 1991. In: Tyson, R.V., Pearson, T.H. (Eds.), Geol. Soc. London Sp. 58, 1–24. https://doi.org/10.1144/GSL.SP.1991.058.01.01.
- Wang, X.N., Li, J.R., Jiang, W.Q., Zhang, H., Feng, Y.L., Yang, Z., 2022. Characteristics, current exploration practices, and prospects of Continental shale oil in China. Advances in Geo-Energy Research 6 (6), 454–459. https://doi.org/10.46690/ager.2022.06.02
- Wang, E.Z., Feng, Y., Guo, T.L., Li, M.W., 2022. Oil content and resource quality evaluation methods for lacustrine shale: A review and a novel threedimensional quality evaluation model. Earth Sci. Rev. 232, 104134. https:// doi.org/10.1016/j.earscirev.2022.104134.
- Wang, E.Z., Feng, Y., Guo, T.L., Li, M.W., Xiong, L., Lash, G.G., Dong, X.X., Wang, T., Ouyang, J.S., 2023a. Sedimentary differentiation triggered by the Toarcian Oceanic anoxic event and formation of lacustrine shale oil reservoirs: organic matter accumulation and pore system evolution of the early Jurassic sedimentary succession, Sichuan Basin, China. J. Earth. Sci. 256, 105825. https://doi. org/10.1016/j.jseaes.2023.105825.

- Wang, E.Z., Guo, T.L., Li, M.W., Xiong, L., Dong, X.X., Wang, T., Li, H.Q., 2023b. Favorable exploration lithofacies and their formation mechanisms in lacustrine shales deposited under different salinity conditions: insights into organic matter accumulation and pore systems. Energy Fuels 37 (16), 11838–11852. https://doi.org/10.1021/acs.energyfuels.3c02038.
- Wang, G.P., Jin, Z.J., Liu, G.X., Wang, R.Y., Zhao, G., Tang, X., Liu, K.Q., Zhang, Q., 2023c. Pore system of the multiple lithofacies reservoirs in unconventional lacustrine shale oil formation. Int. J. Coal Geol. 273, 104270. https://doi.org/10.1016/j.coal.2023.104270.
- Wang, E.Z., Li, M.W., Ma, X.X., Qian, M.H., Cao, T.T., Li, Z.M., Yang, W.W., Jin, Z.J., 2024a. Diahopane and diasterane as the proxies for paleoenvironment, hydrocarbon generation condition, and shale oil accumulation. Chem. Geol. 670, 122447. https://doi.org/10.1016/j.chemgeo.2024.122447.
  Wang, L., Lyu, Q.Q., Li, L.H., Liu, J., Luo, S.S., Sun, X.H., Zhang, L., Xu, X.S., 2024b.
- Wang, L., Lyu, Q.Q., Li, L.H., Liu, J., Luo, S.S., Sun, X.H., Zhang, L., Xu, X.S., 2024b. Sedimentary characteristics of mixed source fine-grained gravity-flow and its significance for shale oil exploration in a lacustrine depression Basin: A case study of the chang 73 Sub-member of the Triassic Yanchang Formation in Ordos Basin, NW China. Sediment. Geol. 464, 106629. https://doi.org/10.1016/j. sedgeo.2024.106629.
- Wei, Z., Zou, Y.R., Cai, Y., Wang, L., Luo, X., Peng, P., 2012. Kinetics of oil group-type generation and expulsion: an integrated application to Dongying Depression, Bohai Bay Basin, China. Org. Geochem. 52, 1–12. https://doi.org/10.1016/j.orggeochem.2012.08.006.
- Wu, Z.Y., Zhao, X.Z., Wang, E.Z., Pu, X.G., Lash, G., Han, W.Z., Zhang, W., Feng, Y., 2021. Sedimentary environment and organic enrichment mechanisms of lacustrine shale: A case study of the Paleogene Shahejie Formation, Qikou Sag, Bohai Bay Basin. Palaeogeogr. Palaeoclimatol. Palaeoecol. 573, 110404. https://doi.org/10.1016/j.palaeo.2021.110404.
- Wu, Z.R., Littke, R., Baniasad, A., Yang, Z., Tang, Z.X., Grohmann, S., 2023. Geochemistry and petrology of petroleum source rocks in the Upper Cretaceous Qingshankou Formation, Songliao Basin, NE China. Int. J. Coal Geol. 270, 104222. https://doi.org/10.1016/j.coal.2023.104222.
- Xu, Z., Liu, L., Liu, B., Wang, T., Zhang, Z., Wu, K., Feng, C., Dou, W., Wang, Y., Shu, Y., 2019. Geochemical characteristics of the Triassic chang 7 lacustrine source rocks, Ordos Basin, China: Implications for paleoenvironment, petroleum potential and tight oil occurrence. J. Asian Earth Sci. 178, 112–138. https://doi.org/10.1016/j.jseaes.2018.03.005.
- Yan, Y., Wang, M., Misch, D., Sachsenhofer, R.F., Wu, Y., Li, J.B., 2024. Mineral diagenesis in lacustrine organic-rich shales: Evolution pathways and implications for reservoir characteristics. J. Asian. Earth. Sci. 263, 106026. https:// doi.org/10.1016/j.jseaes.2024.106026.
- Yang, R.C., van Loon, A.J., 2022. The Ordos Basin: Sedimentological Research for Hydrocarbons Exploration. Elsevier. https://doi.org/10.1016/C2020-0-01240-5.
- You, J.Y., Liu, Y.Q., Li, Y.J., Zhou, D.W., Zheng, Q.H., Yang, Y.Y., Shi, J., Gao, H.F., 2021. Influencing factor of chang 7 oil shale of Triassic Yanchang Formation in Ordos Basin: constraint from hydrothermal fluid. J. Petrol. Sci. Eng. 201, 108532. https://doi.org/10.1016/j.petrol.2021.108532.
- Zhang, M.Z., Ji, L.M., Wu, Y.D., He, C., 2015. Palynofacies and geochemical analysis of the Triassic Yanchang Formation, Ordos Basin: Implications for hydrocarbon generation potential and the paleoenvironment of Continental source rocks. Int. J. Coal Geol. 152 (B), 159–176. https://doi.org/10.1016/j.coal. 2015.11.005.
- Zhang, W.Z., Yang, W.W., Xie, L.Q., 2017. Controls on organic matter accumulation in the Triassic chang 7 lacustrine shale of the Ordos Basin, Central China. Int. J. Coal Geol. 183, 38–51. https://doi.org/10.1016/j.coal.2017.09.015.
- Zhang, J.Q., Qiu, Z., Li, S.T., Gao, S.L., Guo, R.L., Ma, X.F., Qiu, J.L., Li, S.X., Tao, H.F., Chen, J.L., Li, J.C., Xiao, W.J., 2023. Linking environmental changes and organic matter enrichment in the middle part of the Yanchang Formation (Ordos Basin, China) to the rollback of an Oceanic slab in the eastern paleo-tethys. Sediment. Geol. 455, 106480. https://doi.org/10.1016/j.sedgeo.2023.106480.
- Zhao, W.Z., Zhu, R.K., Hu, S.Y., Hou, L.H., Wu, S.T., 2020a. Accumulation contribution differences between lacustrine organic-rich shales and mudstones and their significance in shale oil evaluation. Petrol. Explor. Dev. 47 (6), 1160–1171. https://doi.org/10.1016/S1876-3804(20)60126-X.
- Zhao, Z.B., Littke, R., Zieger, L., Hou, D.J., Froidl, F., 2020b. Depositional environment, thermal maturity and shale oil potential of the Cretaceous Qingshankou Formation in the eastern Changling sag, Songliao Basin, China: an integrated organic and inorganic geochemistry approach. Int. J. Coal Geol. 232, 103621. https://doi.org/10.1016/j.coal.2020.103621.
- Zhao, W.Z., Bian, C.S., Li, Y.X., Liu, W., Qin, B., Pu, X.G., Jiang, J.L., Liu, S.J., Guan, M., Dong, J., Shen, Y.T., 2024. "Component flow" conditions and its effects on enhancing production of Continental medium-to-high maturity shale oil. Petrol. Explor. Dev. 51 (4), 826–838. https://doi.org/10.1016/S1876-3804(24) 60509-4.